Characterization and rescue by oxytocin of an atypical thermo-sensory reactivity in neonatal mice lacking the autism-associated gene *Magel2*.

Laura Caccialupi Da Prato[1], Dina Abdallah[1], Vanessa Point[2], Fabienne Schaller[1], Emilie Pallesi-Pocachard[1], Aurélie Montheil[1], Stéphane Canaan[2], Jean-Luc Gaiarsa[1], Françoise Muscatelli[1], Valéry Matarazzo[1#]

[1] Aix Marseille Univ, INSERM, INMED, Marseille, France

[2] Aix-Marseille Univ, CNRS, LISM, IMM, Marseille, France

#: corresponding author

Email: valery.matarazzo@inserm.fr;

Institut de Neurobiologie de la Méditerranée (INMED)

INSERM-Aix Marseille Université, UMR1249

Campus Scientifique de Luminy, 13273 Marseille, France

Keywords: thermo-sensory; Autism; Schaaf-Yang syndrome, Prader-Willi syndrome; Oxytocin

ABSTRACT

Atypical responses to sensory stimuli are considered as a core aspect and early life marker of autism spectrum disorders (ASD). Although recent findings performed in mouse ASD genetic models report sensory deficits, these were explored exclusively during juvenile or adult period. Whether sensory dysfunctions might be present at the early life stage is unknown. Here we investigated cool thermosensibility during the first week of mouse life. In response to cool temperature exposure control neonates undertake innate behaviors by eliciting low-latency ultrasonic vocalization. However, we found that neonatal mice lacking the autism-associated gene *Magel2* fail to react to cool stimuli while long-term thermoregulatory function, namely nonshivering thermogenesis, is active. Investigation of the sensory pathway revealed abnormal cool-induced response in the medial preoptic area. Importantly, intranasal administration of oxytocin can rescue this thermosensory reactivity. In addition, chemogenetic inactivation in control neonates of hypothalamic oxytocin neurons reproduces the coolness response failure observed in *Magel2* mutants. Collectively, these findings establish for the first-time impairments of thermal lower-reactivity in a mouse model of ASD with deletion of Magel2 gene during early life period and reveal that the oxytocinergic system regulates this neonatal cool thermosensibility.

INTRODUCTION

Autism spectrum disorder (ASD) is a developmental disorder characterized by deficits of social interaction and communication, as well as by repetitive interests and activities. However, atypical sensory behaviors are a core aspect of ASD affecting 90% of children (Robertson and Baron-Cohen, 2017). Importantly, sensory symptoms have been documented as early as 6 months in ASD infants, preceding considerably the common core features (Baranek et al., 2013; Estes et al., 2015). Much of research in animal models of syndromic and non-syndromic forms of ASDs has focused on the social and cognitive difficulties and their underlying mechanisms (Robertson and Baron-Cohen, 2017). Recent increasing evidences suggest that sensory traits such as tactile, visual, auditory, olfactory, gustatory and heat abnormalities (Chelini et al., 2019; Cheng et al., 2017; Drapeau et al., 2018; Huang et al., 2019; Orefice et al., 2016; Siemann et al., 2017) are present in ASD models, yet the existence of sensory dysfunctions during early life period have been unexplored.

During the first week of life, sensory integrity is vital since neonates have to undertake innate behaviors such as nipple-searching and calls in response to sensory stimuli. Among the different stimuli, sensing any reduction of the ambient temperature is particularly relevant for neonatal pups. Indeed, unlike their homeothermic adult counterparts, neonates are poikilothermic (Wixson and Smiler, 1997) and should be keep in close contact with the mother in order to keep their body temperature. In the absence of their warmth-giving mother and being exposed to cool temperatures, neonates generate ultrasonic vocalizations (USV), thereby inducing pup-retrieval and maternal-care behaviors in dams. In fact, during the preweaning period, exposure to low ambient temperatures is considered as a major stimulus for eliciting USV (Blumberg et al., 1992; Oswalt and Meier, 1975b; Szentgyörgyi et al., 2008). This responsiveness is independent of mother separation and declines towards adulthood, which is presumably correlated with the increasing capability of rodents to develop other thermoregulatory behaviors such as seeking comfortable temperature (Allin and Banks, 1971; Blumberg et al., 1992; Oswalt and Meier, 1975a; Szentgyörgyi et al., 2008).

Here we thus investigate for the first time the existence of deficit in thermal sensitivity in neonate mice lacking the *Magel2* gene. *MAGEL2* is an imprinted gene that is paternally expressed and which paternal deletion or mutation is respectively involved in Prader-Willi (Boccaccio et al., 1999) and Schaaf-Yang syndromes (Schaaf et al., 2013) (PWS OMIM #176270 and SHFYNG-OMIM #615547, respectively), two neurodevelopmental diseases characterized with high incidence of ASD features (25% and 78% respectively for PWS and SYS). Both syndromes share overlap phenotype including feeding difficulties and hypotonia

in infancy then alterations in social behavior and deficits in cognition over lifespan. It has been previously shown that *Magel2*-null mouse model mimics early feeding and adult social interaction deficits (Fountain et al., 2017; Meziane et al., 2015; Schaller et al., 2010). Moreover, *Magel2* neonates display deficiencies of hypothalamic oxytocin (OT) neuropeptide and OT treatment can restore these deficits (Meziane et al., 2015; Schaller et al., 2010). Importantly, OT has been found to be a modulator of adult sensory functions (Grinevich and Stoop, 2018). Both adult and young mice lacking a functional OT system have thermogenesis difficulties ((Harshaw et al., 2018; Kasahara et al., 2013; Kasahara et al., 2007; Kasahara et al., 2015; Xi et al., 2017) which affect in response to cold challenge huddling and thermotaxis behavior in the litter (Harshaw et al., 2018)

The neuronal pathways underlying cool response behavior is still under intensive investigation. At the peripherical level, thermosensory neurons have been described in the skin and also in the Grueneberg ganglion – a cluster of sensory neurons localized at the tip of the nose (Bumbalo et al., 2017; Chao et al., 2015; Mamasuew et al., 2008; Mamasuew et al., 2011). Interestingly, the Grueneberg ganglion is functional very early in life since these thermosensory neurons are already wired at birth to necklace olfactory glomeruli (Matsuo et al., 2012) and induces USV in response to cool stimuli (Chao et al., 2015). Deletion of the Grueneberg ganglion thermoreceptors reduces coolness-evoked USV in 2 days aged pups (Chao et al., 2015). At the central level, the preoptic aera (POA) plays a major role sensing and integrating peripheral thermosensory informations (Tan et al., 2016). Moreover, it has been shown in adult mice that activation of the POA modulates USV (Gao et al., 2019).

These findings prompted us also to investigate these peripheral and central regions. In the present study we have used a mouse SHFYNG and PWS genetic model (*Magel2*$^{+/-p}$) combined with neonatal behavioral testing, pharmacology, pharmacogenetics, biochemistry and electrophysiology to demonstrate a lack of cool reactivity behavior during the first week of life. Our findings reveal that alteration of the oxytocinergic system is involved in this sensory deficit.

RESULTS

1- *Deletion of Magel2 exhibits indifference call behavior to cool stimuli during the first week of life*

We first asked whether *Magel2*$^{+/-p}$ neonates exhibit deficits in thermal sensitivity. Male and female neonates wild-type (WT) and *Magel2*$^{+/-p}$ aged from 0 to 6 days old (P0 to P6) were subjected to thermosensory sensitivity.

To assess thermosensitivity in neonates, we developed an experimental procedure based on coolness-induced USV (Chao et al., 2015) (Figure 1A). Littermates were taken from their nests, isolated from the dam, and exposed separately and successively to two different temperatures (25°C and 17°C). This procedure allows us to compare ambient versus cool exposure responses within the same animal. Exposure of pups at birth (P0) elicited a rather low rate of USV compared to the next post-natal days (Figure 1, supplemental 2A); therefore, we excluded this age and focused our analyses from P1 to P6. On analyzing the latency to the first call, which reflects the reactivity of the animals to sense cold, we found that WT neonates presented a low-latency in emitting their first call when exposed to ambient *versus* cool temperatures (P1: 1.56±0.27 ln+1 s *vs* 0.34±0.08 ln+1 s; n=16, p=0.0003; P2: 1.48±0.26 ln+1 s *vs* 0.55±0.13 ln+1 s; n=15, p=0.0054; P3: 2.08±0.32 ln+1 s *vs* 1.19±0.27 ln+1 s; n=15, p=0.0256; Wilcoxon test) (Figure 1 B-E-H-K), while *Magel2*$^{+/-p}$ did not (Figure 1 C-F-I-L). This hyporeactivity in the mutant pups was observed at P1 and P2 (P1: 1.79±0.29 ln+1 s *vs* 0.76±0.29 ln+1 s; n=17, p=0.0984; P2: 1.95±0.31 ln+1 s *vs* 2.14±0.45 ln+1 s; n=15, p=0.4037, Wilcoxon test) (Figure 1 C-F). At P3 and P6 the latencies in emitting the first USV after exposure to 17°C were even higher than to 25°C (P3: 2.5±0.38 ln+1 s *vs* 3.24±0.46 ln+1 s; n=16, p=0.0207; P6: 2.21±0.41 ln+1 s *vs* 3.65± 0.45 ln+1 s; n=13, p=0.0034, Wilcoxon test) (Figure 1 I and L).

Furthermore, the responsive rate to cool temperature (i.e. the proportion of neonates responsive to cooling) was markedly decreased in *Magel2*$^{+/-p}$ from P1 to P6 compared to the WT (P1: WT 87.5±8.5 %, n=16; *Magel2*$^{+/-p}$ 58.82±12.3 %, n=17, p<0.0001; P2: WT: 73.33±11.82 %, n=15; *Magel2*$^{+/-p:}$ 37.5±12.5 %, n=16, p<0.0001; P3: WT 73.33±11.82 %, n=15; *Magel2*$^{+/-p}$ 20±10.69 %, n=15, p<0.0001; P6: WT 50±15.08 %, n=12; *Magel2*$^{+/-p}$ 7.69±7.69 %, n=13, p<0.0001, Fisher's exact test) (Figure 1D-G-J-M).

In order to exclude any potentiation or dam separation effects in our experimental paradigm we run assays in which USV box temperature was kept to 25°C (Figure 1 Supplemental 1A). Using new cohorts of animals, we found that WT performed comparably upon repetitive ambient temperature exposures (Figure 1 Supplemental 1B-C and G-H). Moreover, we run an experimental paradigm inversion in which another cohort of animals was first exposed to 17°C and then to 25°C (Figure 1 Supplemental 1D). WT neonates still presented a low-latency response when exposed to cool *versus* ambient temperatures (Figure 1 Supplemental 1E-F and G-H). Thus, latency of the first call of isolated neonates was dependent on external temperature.

While no difference in latency of the first call and number of USV calls were observed at ambient temperature, only exposure to 17°C evoked a significant and age-dependent difference between WT and *Magel2*$^{+/-p}$ in latency from P2 to P6 (P2: WT 0.96±0.28 s, n=15; *Magel2*$^{+/-p}$ 29.81±11.32 s, n=15; p=0.03 ; P3: WT 5.71±2.26 s, n=15; *Magel2*$^{+/-p}$ 67.15±20.92 s, n=15, p=0.005; P6: WT 19.47±5.90 s, n=12; *Magel2*$^{+/-p}$ 78.69±18.59 n=12, p=0.007, two-way ANOVA, Bonferroni's post-test) (Figure 1O) and in the rate of USV (P2: WT 200.1±29.85 n=16; *Magel2*$^{+/-p}$ 105.2±23.7 %, n=17, p=0.0238; P3: WT 201.6±35.31 %, n=16; *Magel2*$^{+/-p}$ 48.24±10.49, n=17, p<0.0001, two-way ANOVA, Bonferroni's post-test) (Figure 1, supplemental 2B).

Analyses of others USV parameters revealed that call duration was significantly different at 25°C between the two genotypes; *Magel2*$^{+/-p}$ pups having lower call duration at P2, P3 and P6 (P2: WT 29.43±1.89 ms, n=16; *Magel2*$^{+/-p}$ 22.42±1.81 ms n=17, p=0.0289; P3: WT 30.29±1.53 ms, n=16; *Magel2*$^{+/-p}$ 19.25±1.51 ms n=15, p=0.0001; P6: WT 23.47±2.38 ms, n=12; *Magel2*$^{+/-p}$ 14.23±1.28 ms n=11, p=0.0110; two-way ANOVA, Bonferroni's post-test) (Figure 1, supplemental 2C). However, this difference in call duration was not anymore observed upon cool challenge exposure (17°C) (Figure 1, supplemental 2D).

Thus, *Magel2*$^{+/-p}$ neonates exhibited impairments in cool sensitivity behavior during the first week of life. This deficit was independent of the sex since both *Magel2*$^{+/-p}$ males and females exhibited high-latency to the first call and a decreased number of USV calls during cool stimuli (Figure 1, supplemental 2B and E).

As previously observed, we confirmed that the USVs produced by WT pups in response to a cool challenge changed as the pups matured (Kromkhun et al., 2013). Responses of WT pups to cool exposure significantly decrease as their fur growth and their ear canals open at 1 week of age. This is something that we observed in our WT pups since at P6, the latency of the first call after cool exposure started to be non-significant from ambient exposure (2.97±0.39 ln+1 s *vs* 2.56±0.29 ln+1 s, n=12, p=0.3804, Wilcoxon test) (Figure 1K) and the percentage of reactive animals was only 50% (Figure 1N). At P8, USV responses were clearly produced independently of the exposed temperature (data not shown). Thus, this cool thermosensory call behavior which is an innate reflex presents during a short-term period (i.e. the first week of life) was not observedin *Magel2*$^{+/-p}$. We next decided to focus our experiments at P2, an age when the latency of the first call upon cool exposure starts to be significant between *Magel2*$^{+/-p}$ and WT (Figure 1 O).

2- Cool thermosensory call behavior impairment in Magel2$^{+/-p}$ neonates is not correlated with either difference in acute stress-induced dam separation nor difference in cool induced-hypothermia.

Next, we asked whether these deficiencies of *Magel2*$^{+/-p}$ in cool reactivity could account to abnormalities in corticosterone basal levels. In human, cortisol change has been associated to greater sensitivity in autistic children (Corbett et al., 2008). Whilst USVs are not related to corticosterone stress response in isolated rat pups (Klint and Andersson, 1994; Lehmann et al., 2002) and the HPA axis is not fully mature at this developmental age, *Magel2* is expressed in hypothalamic neurons and in the cortical cells of the adrenal glands. oOne can thus still hypothesize that basal levels of corticosterone might be affected in *Magel2*$^{+/-p}$. Using new cohorts, pups were handled similarly than previously except that after dam separation and just before USV recording, they were sacrificed and blood samples were collected (Figure 1A). We found that both male and female *Magel2*$^{+/-p}$ neonates exhibit similar corticosterone levels compared to WT (males: WT: 12,974±6,711 ng/ml, n=6; *Magel2*$^{+/-p}$: 24,328±1,971 ng/ml, n=7, p=0.4740; females: WT 19,983±4,425 ng/ml, n=7; *Magel2*$^{+/-p}$: 28,831±10,314 ng/ml, n=6, p=0.6723, two-way ANOVA, Bonferroni's post-test) (Figure 1P). Thus, dam separation and handling of *Magel2*$^{+/-p}$ did not affect corticosterone levels differently from WT and cannot be the cause of deficiency in cool thermosensory call behavior.

Next, using an infrared thermometer we followed skin body temperature during this acute cool exposure. After removal from the nest for 5 min, the temperatures dropped similarly for WT and *Magel2*$^{+/-p}$. Upon short-term cool exposure (17°C; 5 min), although substantial drop of temperature was observed, the decrease was similar between both genotypes (Figure 1, supplemental 2F). Thus, this last result shows that temperatures of WT and *Magel2*$^{+/-p}$ neonates are similar and evolve similarly upon acute cool exposure.

2- Cool thermosensory call behavior impairment in Magel2$^{+/-p}$ neonates is not caused by deficiency in non-shivering thermogenesis

Following cool exposure experienced in the transition from the uterine to extrauterine environments and also during the first week of life, newborns require an effective thermoregulatory adaptative response to produce heat (Symonds et al., 2015). During this first week, the primary source of heat is produced by the sympathetically mediated metabolism of brown adipose tissue (BAT); also, so called non-shivering thermogenesis (Oelkrug et al., 2015). Activation of this cold-defensive response is dependent on a thermal afferent neuronal signaling, which involved at the periphery thermoreceptors, namely

TRPM8, located in the skin and a spino-parabrachial tractus projecting to the preoptic area of the hypothalamus (Yahiro et al., 2017).

Magel2 being expressed in dorsal root ganglia (Kozlov et al., 2007; Matarazzo and Muscatelli, 2013), we first analyzed whether peripheral expression of TRPM8 could be affected in *Magel2*$^{+/-p}$ compared to WT neonates. We found no significant difference of the TRPM8 transcript (Figure 2 supplemental 1).

In order to investigate whether the cool thermosensory call behavior impairment found in *Magel2*$^{+/-p}$ neonates could be related to dysfunction of non-shivering thermogenesis, we analyzed the BAT tissue since it's the final target of this thermoregulatory pathway. We first found that P2 *Magel2*$^{+/-p}$ had significant decreased interscapular mass BAT compared to aged-matched WT (Figure 2A). However, this difference of mass BAT was inverted at P6 (Figure 2A); the mass BAT declining in WT but not in mutant ones (P2: WT 8.52±0.47 mg/g, n=42; *Magel2*$^{+/-p}$: 5.25±0.26 mg/g, n=40, p<0.0001; P6: WT: 4.66±0.17 mg/g, n=42; *Magel2*$^{+/-p}$: 6.18±0.27 mg/g, n=40, p=0.0045, two-way ANOVA, Bonferroni's post-test).

We found that *Magel2* is expressed in BAT although at a lower level than in the hypothalamus (WT BAT: $1.03x10^{-3}$($4.20x10^{-4}$; $1.53x10^{-3}$), n=12; WT hypothalamus: $3.79x10^{-2}$ ($3.14x10^{-2}$; $4.53x10^{-2}$), n=24) (Figure 2B). Interestingly, *Necdin*, a member from the same family of *Magel2* and also affected in SPW, has been found to be expressed in the BAT and functions as an antiproliferative factor of adipocyte progenitor cells and inhibitor of brown adipocyte differentiation (Cypess et al., 2011; Fujiwara et al., 2012). By analyzing Necdin expression in the *Magel2* mutant mice, we observed at P2 a significant increase both at the RNA (WT: $2.16x10^{-2}$ ($1.66\ x10^{-2}$; $2.95\ x10^{-2}$), n=12; *Magel2*$^{+/-p}$: $3.68x10^{-2}$ ($1.78x10^{-2}$; $4.34\ x10^{-2}$), n=10, p=0.0358, Mann Whitney test) (Figure 2C) and protein levels (WT: 0.29 ($1.24\ x10^{-2}$, 0.53), n=6; *Magel2*$^{+/-p}$: 0.61 (0.48, 0.75), n=4, p=0.0190, Mann Whitney test) (Figure 2D-E). However, this Necdin over-expression was still observed at P6 (WT: 0.64 (0.56; 0.78), n=14; *Magel2*$^{+/-p}$: 1.22 (0.77, 1.34), n=14, p=0.0006, Mann Whitney test) (Figure 2F and G), an age when BAT mass of *Magel2*$^{+/-p}$ is increased compared to age-matched WT. Thus Necdin over-expression cannot be correlated to the loss of BAT mass; and these results are consistent with a previous study showing that *Necdin* deficiency alters proliferation of adipocyte progenitor without affecting BAT mass (Fujiwara et al., 2012).

We next investigated BAT function through the analyses of BAT lipolysis and the mitochondrial expression of the uncoupling protein 1 (UCP1) since fatty acids (FA) activate and fuel UCP1-mediated non-shivering thermogenesis in BAT (Townsend and Tseng, 2012). In order to observe BAT activation, we extracted one hour after cool exposure (17°C) interscapular BAT tissues, a major source of thermogenesis.

Quantitative analyses of BAT lipids, separated by thin layer chromatography (Figure 3A-D), show that although cold exposure induced a significant decrease of triglycerides in both WT and *Magel2*$^{+/-p}$ pups (WT: 1.53.10^{8} (1.27.10^{8}; 1.60.10^{8}), n=8, *vs* 7.93.10^{7} (6.27.10^{7}; 1.31.10^{8}), n=7; *Magel2*$^{+/-p}$: 1.72.10^{8} (1.50.10^{8}; 1.98.10^{8}) *vs* 9.51.10^{7} (8.22.10^{7}; 1.36.10^{8}), n=7, Kruskal-Wallis test Dunn's post-test) (Figure 3E), levels of diglycerides and FA remained surprisingly unchanged for both genotypes (Figure 3E-G). Our observation that BAT FA are not consumed upon cold exposure are consistent with recent findings controverting the current view that BAT-derived FA are essential for thermogenesis during acute cold (Schreiber et al., 2017).

Next, we found that upon acute cool exposure (17°C, 1 h), UCP1 protein expression significantly increases in WT (0.99 (0.48, 1.41), n=6, *vs* 2.03 (1.61, 3.25), n=5, p=0.0173, Mann Whitney test) (Figure 4A and B) as well as *Magel2*$^{+/-p}$ (0.86 (0.71, 1.95), n=11, *vs* 2.49 (1.56, 4), n=11, p=0.0104, Mann Whitney test) (Figure 4C and D). Similar results were observed at the age of P6 (WT: 0.62 (0.57; 0.89), n=6, *vs* 3.84 (2.31; 4.64), n=6, p=0.0043; *Magel2*$^{+/-p}$: 0.38 (0.32; 0.58), n=6, *vs* 3.12 (2.11; 4.29), n=6, p=0.0022, Mann Whitney test) (Figure 4E-H). Thus, these results demonstrate that UCP1-mediated nonshivering thermogenesis in BAT is fully active in *Magel2* deficient pups. They are also consistent with recent findings showing that UCP1 activation is independent of BAT mass and BAT-derived FA (Schreiber et al., 2017). Altogether, our results demonstrate that lack of cool thermosensory call behavior found in *Magel2* deficient pups is not related to their capacity of regulating temperature.

3- Magel2$^{+/-p}$ *thermosensitive neurons from the Grueneberg ganglion are responding to cool stimulation*

The Grueneberg ganglion (a region located at the tip of the nose) contains sensitive neurons responding to cool temperatures (Mamasuew et al., 2008) and it has been proposed to influence USV (Fleischer and Breer, 2010) generated by rodent pups to elicit maternal care on exposure to cool temperatures (Blumberg et al., 1992; Hashimoto et al., 2004; Szentgyörgyi et al., 2008). Interestingly, mice pups deleted for the thermoreceptor expressed in these sensory neurons present USV calls impairment after cool exposure; a phenotype very similar to what we observe here in *Magel2*$^{+/-p}$ (Chao et al., 2015). We thus ask whether these peripheral sensory neurons might be affected in *Magel2*$^{+/-p}$. We conducted calcium bi-photon imaging on tissue slices through the Grueneberg ganglion of P2 neonates which was identified by its specific location, morphology and Fura 2AM loading (Figure 5A-B). Thermo-evoked neuronal activities (obtained by decreasing the temperature of the perfusion solution from 37 to 15°C) elicited a substantial increase in intracellular Ca^{2+} in both all WT and *Magel2*$^{+/-p}$ animals tested (Figure 5 C). Although differences in the percentage of responding

cells might exist between WT and *Magel2*$^{+/-p}$ neonates, the Grueneberg ganglion thermosensory neurons were functional in the mutant mice.

4- Thermo-evoked response of medial preoptic area neurons is altered in Magel2$^{+/-p}$ *neonates*

Within the hypothalamus, the medial preoptic area (mPOA) is the primary site in which a variety of sensory information, including temperature, is integrated to modulate the descending command outputs, including USV (Gao et al., 2019).The mPOA also contains thermosensitive neurons whose firing rates change upon elevating or reducing local tissue mPOA temperature (Boulant, 1986; Nakayama et al., 1961; Tan et al., 2016).

We thus ask whether the response of central thermo-sensitive neurons of the mPOA might be affected in *Magel2*$^{+/-p}$. We prepared acute hypothalamic slices from P2 neonates and recorded the multi-unit activity in the mPOA (Figure 6A). Decreasing the temperature of the perfusion solution from 35 to 30°C elicited a substantial and reversible increase in the firing rate of mPOA neurons in 5 out of 7 of WT mice (Figure 6B-D). The firing frequency was (0.95±0.45 Hz at 35°C and 1.62±0.71 Hz, n=5, p=0.0625, Wilcoxon test) after switching to 30°C. In the 2 remaining mice, decreasing the temperature decreased the firing rate of mPAO neurons (from 0.64±0.26 Hz to 0.32±0.04 Hz). In contrast, the same protocol elicited a significant decrease in the firing rate of PAO neurons in 5 out of 8 *Magel2*$^{+/-p}$ mice (from 0.84±0.17 Hz to 0.37±0.09 Hz, p=0.04, Figure 6B-D). In the 3 remaining slices, the firing frequency was increased from 0.36±0.17 Hz to 1.08±0.34 Hz. Altogether, these results show that thermo-evoked response of mPAO neurons is altered in *Magel2*$^{+/-p}$ mice.

5- Intranasal injection of Oxytocin rescues cool sensitivity call behavior in Magel2+/-p neonates

Oxytocin (OT) is a main neuropeptide involved in mediating the regulation of adaptive interactions between an individual and his environment (Muscatelli et al., 2017); in major part by modulating sensory systems (Grinevich and Stoop, 2018). Furthermore, previous studies demonstrated efficacy of OT to improve suckling, cognitive or social behaviors in genetic models of neurodevelopmental disorders (Harony-Nicolas et al., 2017; Meziane et al., 2015; Peñagarikano et al., 2015; Schaller et al., 2010). We thus ask whether OT could improve thermosensory call behavior in the *Magel2*$^{+/-p}$ neonates during neonatal period (P2). Of the two preferred route to reach CSF, and considering the small size of mice pups, we found more convenient to administrate OT by intranasal (IN) rather than intravenous route (Lee et al., 2018). New cohorts of neonatal pups were tested for cool thermosensory call behavior with a similar procedure excepted that neonates received the treatment in between ambient

and cool exposures. This procedure allows us to analyze the effect of an acute OT treatment by comparing ambient *versus* cool exposure responses within a same animal (Figure 7A).

We first verified that handling and IN administration procedures did not affect cool-induced call behavior of *Magel2*$^{+/-p}$ neonates by comparing untreated and vehicle-treated groups. After vehicle treatment (saline solution), *Magel2*$^{+/-p}$ were still unable to react to cool exposure since the latency to the first call in cool exposure was similar to ambient exposure (2.83±0.39 ln+1 s *vs* 2.64±0.43 ln+1 s, n=9, p=0.9102, Wilcoxon test) (Figure 7B). Furthermore, comparison of the cooling rate reactivity (37.5±12.5 % n=16 *vs* 40±16.33 %, n=9, p=0.7714, Fisher's exact test) or the number of USV calls revealed insignificant change between these control groups (105.2±23.7, n=17 *vs* 41.3±16.48, n=10, p=0.6561, Kruskal-Wallis test Dunn's post-test) (Figure 7C and J).

We found that IN administration of OT (2 µg) was able to rescue the cool thermosensory call behavior of *Magel2*$^{+/-p}$ since the latency of the first call was significantly decreased after cool exposure (2.03± 0.39 ln+1 s; 0.59±0.25 ln+1 s, n=13, p=0.0049, Wilcoxon test) (Figure 7D) and the responsive rate to cool temperature (i.e. the proportion of neonates responsive to cooling) was markedly increased in *Magel2*$^{+/-p}$ (*Magel2*$^{+/-p}$ vehicle: 40±16.33 %, n=9; *Magel2*$^{+/-p}$ OT: 76.92±12.16 %, n=13, p<0,0001, Fisher's exact test) (Figure 7E). Indeed, 77% of *Magel2*$^{+/-p}$ reacted to cool stimuli, a percentage similar to the P2 WT (Figure 1G).

To better characterize the pathway implicated in the rescue of the cool-induced call behavior, we tested OT agonist. OT and AVP are closely related nonapeptides that share high sequence and structure homology, differing by only two amino acids in position 3 and 8 (Wallis, 2012) Although only one receptor exists for OT in mammals, there are three different receptors for AVP: V1a, V1b, and V2, the V1a receptor being the predominant form in brain. AVP can also bind and activate the OT receptor (Manning et al., 2012). Among the different agonist developed for the OT receptor, [Thr^4,Gly^7]OT also referred to as TGOT, has been widely used as a selective OT agonist (Manning et al., 2012); We thus treated *Magel2*$^{+/-p}$ neonates (P2) with either AVP or TGOT and performed USV call recording 10 min after administration of the agonist dose. Analyzing the reactivity of the animals to sense cool temperature (the latency to the first call), we found that *Magel2*$^{+/-p}$ neonates (P2) presented a significant faster reaction in emitting their first call when exposed to cool *versus* ambient temperature (*Magel2*$^{+/-p}$ TGOT: 1.54±0.31 ln+1 s *vs* 0.47±0.18 ln+1 s, n=13, p=0.0061; *Magel2*$^{+/-p}$ AVP: 1.44±0.39 ln+1 s *vs* 0.28±0.16 ln+1 s, n=8, p=0.0156, Wilcoxon test) (Figure 7F and H). Furthermore, the responsive rate to cool temperature (i.e. the proportion of neonates responsive to cooling) was markedly increased in *Magel2*$^{+/-p}$ (*Magel2*$^{+/-p}$ vehicle: 40±16.33 %, n=9 *vs* *Magel2*$^{+/-p}$ TGOT: 69.23±13.32 %, n=13, p<0.0001 and *vs* *Magel2*$^{+/-p}$

AVP: 75±16.37 %, n=8, p<0.0001) (Figure 7G-I); reaching similar values as the P2 WT (Figure 1G and I).

Finally, *Magel2*$^{+/-p}$ pups treated either with AVP or TGOT evoked substantial USV call number upon cool exposure (Magel2$^{+/-p}$ vehicle: 41.30±16.48 %, n=10; Magel2$^{+/-p}$ TGOT: 198.50±23.45 %, n=13, p=0.0021; Magel2$^{+/-p}$ AVP: 205.30±44.03 %, n=10, p=0.0103, Kruskal-Wallis test, Dunn's post-test) (Figure 7J), with values similar to WT (WT: 200.1±29.85 %, n=16 *vs* Magel2$^{+/-p}$ TGOT and Magel2$^{+/-p}$ AVP *vs* WT p>0.9999 Kruskal-Wallis test, Dunn's post-test) (Figure 1, supplemental 1B).

Although we cannot exclude a minor contribution of the AVP receptors, these data suggest that the rescue of cool thermosensory call behavior is mainly due to activation of the OT receptors.

WT neonates treated with TGOT have a shorter latency of the first call (WT untreated 1.48±0.26 ln+1 s *vs* 0.55±0.13 ln+1 s, n=15, p=0,0054; WT TGOT: 1.71± 0.37 ln+1 s *vs* 0.16± 0.05 ln+1 s, n=11, p=0.0049, Wilcoxon test) (Figure 7, supplemental 1 A-B). However this treatment resulted in similar responsive rate to cool temperature (WT untreated: 73.33±11.82 % n=15; WT TGOT: 81.82±12.20 %, n=11, p=0.2393, Fishers's exact test) and similar number of USV upon cool temperature (17°C) (WT untreated: 200.1±29.85 %, n=16; WT TGOT: 255.5±39.92 %, n=11, p=0.5039, Mann Whitney test) (Figure 7 supplemental 1 C and D).

6- Oxytocin rescues *Magel2*$^{+/-p}$ brain Erk signaling impairment after cool stimuli

Because cool exposure or stress alters the Erk pathways in the brain by reducing Erk activation (Lee et al., 2016; Whittington et al., 2013) and OT has been shown to block this alteration (Lee et al., 2016), we first examined whether this signaling pathways might be altered in *Magel2*$^{+/-p}$ brain neonates. Erk/P-Erk levels were measured from P2 whole brains of WT and *Magel2*$^{+/-p}$ immediately after ambient or cool exposure. Cytoplasmic levels of P-Erk revealed that brain of WT neonates had a significant cool-induced reduction of P-Erk (0.47±0.07 *vs* 0.16±0.03, n=6, p=0.0022, Mann Whitney test) (Figure 8A and C); while *Magel2*$^{+/-p}$ did not (0.56±0.03, n=7 *vs* 0.58±0.07, n=5, p=0.7424, Mann Whitney test) (Figure 8B and D). More importantly, IN administration of OT prevents the cool-induced reduction of P-ErK in the brain of *Magel2*$^{+/-p}$ (*Magel2*$^{+/-p}$ vehicle: 1.08±0.09; *Magel2*$^{+/-p}$ OT: 0.62±0.12, n=6, p=0.0087, Mann Whitney test) (Figure 8F and H) without affecting the reduction of P-ErK in the brain of WT (WT vehicle: 1.32±0.11, n=5; WT OT: 0.76±0.1, n=4, p=0.0317, Mann Whitney test) (Figure 8E and G). Thus, these results highlight a deficit in the brain of *Magel2*$^{+/-p}$ neonates and reveal that OT's ability to reverse cool thermosensory call behavior may act, at least partly, through Erk pathway.

7- Neonatal inactivation of oxytocinergic neurons of the hypothalamus leads to impaired cool sensitivity call behavior.

To confirm the pharmacological evidence that OT modulates cool sensitivity call behavior and directly test the hypothesis that OT neurons regulate this innate behavioral, we assessed whether inactivation of oxytocinergic neurons of WT hypothalamus neonates can mimic thermosensory impairment observed in *Magel2*$^{+/-p}$ using DREADD (Designer Receptors Exclusively Activated by Designer Drugs) technology (Zhu et al., 2016). We expressed a modified muscarinic acetylcholine receptor tagged with the fluorescent marker mCherry (hM4Di-mCherry), in OT neurons by means of mice bread crossing (Figure 9A). This DREADD receptor can be activated by the ligand clozapine N-oxide (CNO) and its metabolite, clozapine; both drugs crossing the BBB (Jendryka et al., 2019). We restricted hM4Di-mCherry expression to OT neurons by crossing hM4Di-mCherry mice (named here hM4Di) with OT Cre mice in order to drive the expression with the OT promoter (Figure 9B). These mice were called here OT hM4Di.

Vehicle or CNO was injected into P2 neonates by intraperitoneal (IP) administration 2h before starting thermo-sensory behaviors (Figure 9C). We found that vehicle-treated DREADDs-expressing animals, OT hM4Di, presented a significant faster reaction in emitting their first call when exposed to cool *versus* ambient temperatures (3.39±0.3 ln+1 s *vs* 0.78±0.32 ln+1 s, n=7, p=0.0313, Wilcoxon test) (Figure 9D); while CNO-treated OT hM4Di did not (1.97±0.52 s *vs* 1.65±0.54 ln+1 s, n=9, p=0.8203, Wilcoxon test) (Figure 9E). Furthermore, the animal responsive rate to cool temperature was markedly decreased in CNO-treated OT hM4Di with percentages reaching similar values than *Magel2*$^{+/-p}$ neonates (OT hM4Di + CNO: 36.36±15.21 %, n=11; *Magel2*$^{+/-p}$: 37.5±12.5 %, n=16) (Figure 9F). However, CNO treatment did not affect the numbers of USV calls of OT hM4Di neonates either at ambient (25°C) or cool temperature (17°C); the number of USV calls being similar to *Magel2*$^{+/-p}$ neonates (Figure 9 G-H).

To test for any possible effects of CNO that were not DREADDs mediated, CNO was administered either to non-DREADDs-expressing (hM4Di mice not crossed with OT cre mice) or WT P2 neonates. We found that the responsive rate to cool temperature was damped after CNO administration in WT and in CNO-treated non-DREADDs expressing (WT: 73.33±11.82 %, n=15; WT CNO: 43.75±12.81 %, n=16, p<0.0001; OT hM4Di vehicle: 85.71±14.29 %, n=7; hM4Di CNO: 50±16.67 ln+1 s, n=10, p=0.0631, Fisher's exact test)

(Figure 9F), while the number of USV calls remained similar either at ambient (25°C) or cool temperature (17°C) (Figure 9G and H). However, comparisons of the CNO-treated hM4Di with CNO-treated OT hM4Di neonates revealed that the responsive rate to cool temperature of CNO-treated DREADDs-expressing neonates was still significantly lower than CNO-treated non-DREADDs-expressing neonates (OT hM4Di CNO: 36.36±15.21 %, n=11; hM4Di CNO: 50±16.67 %, n=10, p=0.0315, Fisher's exact test) (Figure 9F). Thus, beside a side effect of CNO which has been reported in other behavioral tests (Ilg et al., 2018), our results revealed that *in vivo* inactivation of OT neurons prevents neonates to respond to cool temperature and confirm that OT system can regulate cool sensitivity call behavior.

DISCUSSION

ASD research has mainly focused on ASD-related genes and their impact on social and cognitive behavior in adult. However, atypical sensory reactivity represents early markers of autism and are predictive of social-communication deficits and repetitive behaviors in childhood. Although recent findings performed in mouse ASD genetic models report sensory deficits(Chelini et al., 2019; Cheng et al., 2017; Drapeau et al., 2018; Huang et al., 2019; Orefice et al., 2016; Siemann et al., 2017), they were explored during juvenile or adult period. Whether sensory dysfunctions might be present at the early life stage is something unknown. Here we provide the first experimental evidence that newborn harboring deletion in *Magel2*, *a* gene implicated in PWS and SHFYNG, two syndromes presenting ASD phenotype, exhibit atypical sensory behavior during their first week of life.

With the aim to investigate a relevant sensory function during early life, we explored the thermosensory function. Indeed, sensing any reduction of the ambient temperature is particularly vital, since neonates are poikilothermic. In contrast to adult who can adopt diverse strategies in response to cool stimuli such as thermoregulatory behavior and shivering thermogenesis, newborns need to stay with their warmth-giving mother. In absence of this warming, cool exposure elicits an innate behavior characterized by USV emissions. Here we found that deletion of *Magel2* leads to a hyporeactivity in emitting the first call when neonates are isolated from their dam and exposed to cool temperature. This call reactivity deficit is specific to cool exposure and is not the result of acute dam separation. Moreover, we demonstrate that alteration of the oxytocinergic system is causing this thermo-sensory hyporeactivity.

By exploring possibilities of peripheral and central origins of this deficit, we found BAT activation upon cool challenge, suggesting that the autonomic neural circuit including thermosensory neurons of dorsal root ganglion controlling non-shivering thermogenesis is not affected. Furthermore, investigation of the Grueneberg ganglion, a thermosensory

system present at the tip of the nose, revealed that this peripheral cool sensor is functionally active. However, we cannot completely exclude a peripheral issue through a dysfunction of the trigeminal ganglion since it contains thermosensory neurons detecting orofacial cold stimuli (Morrison and Nakamura, 2019). The nasal branch of the trigeminal nerve also expresses OT receptors that can be activated after IN administration of OT (Murata et al., 2011; Quintana et al., 2018; Tzabazis et al., 2016).

Magel2$^{+/-p}$ neonates might encounter not only difficulties in detecting but also in integrating thermo-sensory stimuli. We provided some evidences for the hypothesis of a central origin. We found first an electrophysiological alteration of the mPOA independently of sensory input stimulations, second a lack of cool-induced alteration of brain pERK signaling and third we showed that brain inactivation of OT neurons in WT reproduces atypical thermo-sensory reactivity.

In adults, mPOA integrates environmental temperature through peripheral inputs, but also intracranial temperature through local mPOA thermo-sensory neurons acting as thermosensors of brain temperature fluctuations (Siemens and Kamm, 2018). Moreover this hypothalamic region has been recently found to modulate USV calls in adults (Gao et al., 2019). Thus the mPOA appears to be a key node in the neonate to conduct cool thermo-sensory call behavior and lack of *Magel2* which is mainly expressed in the hypothalamic region (Kozlov et al., 2007) might alter mPOA functioning.

The fact that OT treatment through IN administration in *Magel2*$^{+/-p}$ is able to rescue this atypical thermosensory behavior and that brain inactivation of OT neurons in WT reproduces this behavior demonstrate a new pivotal role of the oxytocinergic system in modulating early life thermosensory function (Muscatelli et al., 2017). In support to this major role of OT, we have provided previous evidences that the oxytocinergic system is altered in *Magel2*$^{+/-p}$ mice and that early OT treatment restores normal sucking activity, social and cognitive behaviors in adult mice (Meziane et al., 2015; Schaller et al., 2010).

Although cool-induced cry has been also observed in newborn infants more than 20 years ago (Petrikovsky et al., 1997), it is rarely observed nowadays because maintaining the body temperature of the neonate has been emphasized. Measures of early life sensory behavior such as cool-thermosensory call behavior might represent promising avenues for early diagnostic and OT treatment could be considered for therapeutic interventions of this atypical sensory reactivity.

ACKNOWLEDGMENTS

We thank Antonin Vinck and Emmanuelle Brot for their technical help and the members of the animal facility, genotyping and imaging platforms of INMED laboratory. This study has been supported by INSERM, Aix-Marseille Univ., Foundation Lejeune (N°R15117AA) and ANR (PRADOX N°14-CE13-0025) grants. L.C was supported by a PhD fellowship from the French Minister for Research and Technology and from the support of A*MIDEX/ANR (Neuro*AMU Neuroschool PhD program) funded by the French Government « Investissements d'Avenir » program. The authors declare no competing financial interests.

MATERIAL AND METHODS

Animals

Mice were handled and cared in accordance with the Guide for the Care and Use of Laboratory Animals (N.R.C., 1996) and the European Communities Council Directive of September 22th, 2010 (2010/63/EU, 74). Experimental protocols were approved by the institutional Ethical Committee Guidelines for animal research with the accreditation no. B13-055-19 from the French Ministry of Agriculture. All efforts were made to minimize the number of animals used. Magel2 deficient mice were generated as previously described (Schaller et al., 2010). Mice colonies were maintained on the C57BL/6J background except for the B6N.129-Gt(ROSA)26Sor$^{tm1(CAG-CHRM4*,-mCitrine)Ute}$ also known as R26-LSL-hM4Di DREADD which are maintained on a C57BL/6N background, for convenience these mice will be called hM4Di DREADD mice. Due to the parental imprinting of *Magel2* (paternally expressed only) only heterozygous mice (+m/-p) with the mutated allele transferred by the male were used for experiments. These mice were obtained by cross between wild type C57BL/6J females and homozygous males (-m/-p). Homozygous males were obtained by the cross of males (-m/+p) and females (-m/+p). The hM4DI DREADD were generated as previously described (Zhu et al., 2016) and obtained from the Jackson Laboratory (stock #026219). The OT-cre mice also known as Oxytocin-IRES-cre mice were generated as previously described (Wu et al., 2012) and obtained from the Jackson Laboratory (stock #24234). In our experiment we used hM4Di DREADD homozygous // heterozygous OT cre mice (referred as OT hm4DI in this article). And to obtain this genotype, homozygous hM4Di DREADD females were bred to homozygous hM4Di DREADD // heterozygous OT cre males, 50% of the offspring will have the right genotype.

All mice were genotyped by PCR starting from DNA extracted from tail snips, using the following couple of primers:

Ml2KO F Ml2KO R	5'-CCCTGGGTTGACTGACTCAT-3' 5'-TCTTCTTCCTGGTGGCTTTG-3'	To discriminate the mutant allele from the WT one
71456 F 71457 R	5'-CACTCGATCACGTATGGCTCCATCA-3' 5'-GATGGCAGGCACTGACTTACATGCTG-3'	To discriminate the heterozygous from the homozygous mice
hM4Di DREADD F hM4Di DREADD R OlMR9020 OlMR9021	 5'-TCATAGCGATTGTGGGATGA-3' 5'-CGAAGTTATTAGGTCCCTCGAC-3' 5'-AAGGGAGCTGCAGTGGAGTA-3' 5'-CCGAAAATCTGTGGGAAGTC-3'	To detecting the presence of the conditional allele
Cre F Cre R	5'-GCATTACCGGTCGATGCAACGAGTGATGAG-3' 5'-GAGTGAACGAACCTGGTCGAAATCAGTGCG-3'	

Reverse transcription and real time quantitative PCR

Wild-type and mutant newborns were sacrificed at P2 (between 2pm and 4pm). The hypothalamus,brown adipose tissues and dorsal root ganglia were quickly dissected on ice and rapidly frozen in liquid nitrogen, then stored at -80°C. Total RNA was isolated using the RNeasy® Mini Kit (Qiagen, cat #74104), according to the manufacturer's protocol and cDNAs were obtained by reverse transcription using QuantiTect® Reverse Transcription Kit (Qiagen, cat #205311), starting with 600 ng of total RNA.

For quantitative Real-Time PCR, the cDNA samples were diluted 1/10 and amplified in duplicate on LightCycler 480 instrument (Roche). Samples were subjected to PCR amplification using 5 µM of each primer. As housekeeping genes, HPRT was used as reference gene and amplified in parallel. Samples were subjected to a melting curve analysis to confirm the amplification specificity. Results were elaborated with LightCycler 480 Software (version 1.5.0.39).. Target genes (Necdin and Magel2 C-ter,) were normalized on the reference genes.

The sequences of the primer pair used were:

qRT-Necdin S qRT Necdin AS	5'-CTTCACATAGATGAGGCTCAGGAT-3' 5' AACAACCGTATGCCCATGA-3'
qRT-Magel2 C-ter S qRT-Magel C-ter AS	5'-TGCGGAGTGTAGAGGGATTC-3' 5'-CTGGGAGATTCAGAGGGCTA-3'
qRT- HPRT S qRT-HPRT AS	5'-GCCTAAGATGAGCGCAAGGTTG-3' 5'-ACTAGGCAGATGGCCACAGG-3'
qRT- TRPM8 S qRT-TRPM8 AS	5'-GGTTCCCAGTGACGTGGATA-3' 5'-CTCATTTCCCGAGAAGGTACA-3'

Animals' treatment

WT and *Magel2*+/-p neonates were injected 10 min before each experiment; they were gently removed for their mother, placed on a heating pad and given an intranasal injection (IN). The solutions injected were isotonic saline (10 µl) for the control mice and 2 µg of OT (Phoenix Pharmaceuticals Inc., cat #051-01) or 0.2 µg (Thr□,Gly□)-Oxytocin(TGOT) (BACHEM, lot #1062174) or 0.25 µg of Vasopressin (Phoenix Pharmaceuticals Inc., cat #065-07) diluted in isotonic saline (10 µl) for the treated mice. The treatment was performed at day 2 of life (P2).

CNO (Clozapine-N-oxide; Sigma-Aldrich, St Louis, MO, USA) was dissolved in dimethyl sulfoxide (DMSO; Sigma-Aldrich, St Louis, MO, USA) and diluted with 0.9% isotonic saline to volume, the DMSO concentrations in the final CNO solutions were 0.5%. The dose of CNO was 10 mg/kg. CNO were injected sub cutaneous at a volume of 20 µl/2 g body weight. We injected P2 mice 2 h-2 h30 before the experiment.

Temperature

The body surface temperature was measured using an infrared medical thermometer. Temperature's values were taken every 30 sec during 5 min at room temperature (25°C) and every 30 sec during 5 min at 17°C.

Lipids analysis

The brown adipose tissue was extracted from the back of 2 days old WT and Magel2-KO mice. Samples was cut with a scalpel, further incubated with 500 µL of Chloroform/Methanol ($CHCl_3$:CH_3OH, 2:1 *V/V*) solution and stirred for 15 min. Organic and aqueous phase were separated by centrifugation at 10,000 rpm and the organic phase was recovered. Remaining tissue in the aqueous phase was extract two more

times. All organic phases were pooled, washed by 0.2 vol of 0.9% NaCl solution and after centrifugation the organic phase was dried over $MgSO_4$, and then concentrated under nitrogen stream.

Then 19 µL of CH_2Cl_2 were added per mg of brown adipose tissue. For TAG analysis, 2 µL of extract containing total lipids were separated on TLC (Silica Gel 60, Merck) by using petroleum ether:diethyl ether (90:10, *v/v*) as eluent. For DAG, MAG and FA analysis, 5 µL of the same samples were separated on TLC by using heptane:diethyl ether:formic acid (55:45:1, v/v/v) as eluent. The TLC plates were sprayed with a solution of 5% phosphomolybdic acid in ethanol followed by heating at 120°C in an oven for 5-10 min, to visualize the spots.

Each resolved plate was scanned using a Chemidoc™ MP Imaging System (Bio-Rad), and densitometric analyses were performed using the ImageLab™ software version 5.0 (Bio-Rad) to determine relative TAG content per sample.

Corticosterone immunoassay

P2 mice were separated from their mother and placed on a heating pad for 5 min., then sacrificed and blood samples were quickly collected. Blood serum was separated by centrifugation (5,000 rpm, 20 min) and stored at -80°C. Serum corticosterone concentrations were measured with corticosterone ELISA kit (Enzo Life Sciences, Farmingdale, NY, USA) according to the manufacturer's instructions.

Protein extraction and Western blotting

Brain and brown adipose tissues from Magel2$^{+/-p}$ and WT mice were homogenized in RIPA buffer (Thermo Fisher Scientific) with phosphatase and protease inhibitor cocktails (Pierce Protease and Phosphatase Inhibitor Mini Tablets, EDTA-Free) added with 1% Triton (Euromedex, life sciences products) for the brown adipose tissues. Proteins were run on polyacrylamide gel (Bolt 4-12% Bis Tris plus, Invitrogen by Thermo Fisher Scientific), transferred to a nitrocellulose membrane (GE Healthcare Life Science), blocked with 5% Albumine from bovine serum for 30 min-1 h, incubated with primary antibodies against UCP1 (1:1000, Cell Signalling technology, #14670), p44/42 MAPK (1:1000, Cell Signalling technology, #9102), phospho-p44/42 MAPK (1:1000, Cell Signalling technology, #9101) in 5% Albumine from bovine serum, at 4°C overnight, and then incubated with horse radish peroxidase (HRP)-conjugated anti-rabbit IgG (1:2000, Agilent Dako) diluted in 5% Albumine from bovine serum at room temperature for 2 h. Signals were detected using Super Signal West Pico (Thermo Fisher Scientific, #34080) and bands were analyzed with ImageJ.

Calcium imaging

Coronal slice (500 µm section thickness) were prepared from P2 mice pups. Slices were immersed into ice-cold (2-4°C) artificial cerebrospinal fluid (ACSF) with the following composition (in mM): 126 NaCl, 3.5 KCl, 2 $CaCl_2$, 1.3 $MgCl_2$, 1.2 NaH_2PO_4, 25 $NaHCO_3$ and 11 glucose, pH 7.4 equilibrated with 95% O_2 and 5% CO_2. Grueneberg ganglion coronal slices were cut with a vibrating microtome (Leica VT 1000s, Germany) in ice cold oxygenated choline-replaced ACSF and were allowed to recover at least 90 min in ACSF at room (25°C) temperature. Slices were incubated with 10 µM of Fura-2-AM (Life technologies) added with Pluronic acid and dissolved in DMSO, for 45 min at 33°C in an oxygenated aCSF dark chamber. Then the slices were washed with aCSF for 30 min and transferred to a submerged recording chamber perfused with oxygenated (95% O_2 and 5% CO_2) ACSF (3 ml/min) at 30°C. The chamber was first filled with warm (30°C) aCSF for 1 min, then perfused with cool (15°C) aCSF for 3 min and then warm with aCSF for 1 min. Images were acquired every 5 sec with an Olympus BX61WI microscope equipped with a multibeam multiphoton pulsed laser scanning system (LaVision BioTecs) as previously described (Crépel et al., 2007). Images were acquired through a CCD camera, which typically resulted in a time resolution of 50–150 ms per frame. Slices were imaged using a 20×, NA 0.95 objective (Olympus). Imaging depth was on average 80 µm below the surface (range: 50–100 µm). Images were collected by CCD-based imaging system running ImspectorPro software (LaVision Biotec) and analyzed with Fiji software (Schindelin et al., 2012).

USV recording

On the day of testing (P0, P1, P2, P3 and P6), each pup was separated from its littermates and dam after 30 min of habituation to the testing room, placed on a heating pad and each pup were isolated in an box (23 × 28 × 18 cm) located inside an anechoic box (54 × 57 × 41 cm; Couldbourn instruments, PA, USA) for a 5 min test at room temperature (25°C). Then the pup goes back to the dam for 5-10 min and submits a second separation, placed on a heating pad and the USV were recorded during 5 min under cool temperature (17°C). An ultrasound microphone (Avisoft UltraSoundGate condenser microphone capsule CM16/CMPA, Avisoft bioacoustics, Germany) sensitive to frequencies of 10–250 kHz was located in the roof of the isolation box. Recordings were done using Avisoft recorder software (version 4.2) with a sampling rate of 250 kHz in 16 bit format. Data were transferred to SASLab Pro software (version 5.2; Avisoft bioacoustics) and a fast Fourier transformation was conducted (256 FFT-length, 100% frame, Hamming window, and 75% time window overlap) before the analysis. Recordings were analyzed for the number of calls during the 5 min recording at 25°C and 17°C and for the latency which is the first ultrasound call of the

record. The cooling responsive rate was calculated as the proportion of pups responsive to cooling: a pup is responsive if the latency is two time shorter at 17°C than 25°C.

Hypothalamic slice preparation and electrophysiological recordings

Brains were removed and immersed into ice-cold (2-4°C) artificial cerebrospinal fluid (aCSF) with the following composition (in mM): 126 NaCl, 3.5 KCl, 2 $CaCl_2$, 1.3 $MgCl_2$, 1.2 NaH_2PO_4, 25 $NaHCO_3$ and 11 glucose, pH 7.4 equilibrated with 95% O_2 and 5% CO_2. Hypothalamic slices (500 µm thick) were cut with a vibrating microtome (Leica VT 1000s, Germany) in ice cold oxygenated choline-replaced ACSF and were allowed to recover at least 90 min in ACSF at room (25°C) temperature. Slices were then transferred to a submerged recording chamber perfused with oxygenated (95% O_2 and 5% CO_2) ACSF (3 ml/min) at 34°C.Extracellular field potentials were recorded using tungsten wire electrodes (diameter: 50 µm, California Fine Wire, Grover Beach CA, USA) and a low-noise multichannel DAM-8A amplifiers (WPI, GB; lowfilter: 0.1 Hz; highfilter: 3 kHz; ×1000). The signals were digitized using a Digidata1440A convertor (Axon Instruments, USA). pCLAMP1 0.0.1.10 (Axon Instruments, USA) and MiniAnalysis 6.03 (Synaptosoft, Decatur, CA, USA) programs were used for the acquisition and analysis. The neuronal activity was measured at 35°C during 10 to 15 min and then the aCSF was maintained at 30°C. The medium temperature in the recording chamber was measure with a temperature controller TC-324B (Warner Instrument, USA). The rate of medium temperature change in the chamber was 3°C/min.

Statistical analysis

Analysis were performed using two-tailed non parametric statistical tools when the size of the samples was small (GraphPad, Prism 6 software) and the level of significance was set at P<0,05. Values are indicated as following: (Q2 (Q1, Q3), n, p-value, statistical test) where Q2 is the median, Q1 is the first quartile and Q3 is the third quartile and scatter dot plots report Q2 (Q1, Q3), histograms report the mean±SEM. Appropriate tests were conducted depending on the experiment and are indicated in the text or figures legends or supplementary. Mann-Whitney (MW) non-parametric test was performed to compare two unmatched groups and Wilcoxon- Mann-Whitney (WMW) non-parametric test was performed to compare two matched groups. Kruskal-Wallis (KW) followed by a post hoc test Dunn test was performed to compare three or more independent groups. Two-way ANOVA followed by Bonferroni post-hoc test was performed to compare the effect of two factors on unmatched groups. Fisher's exact test was performed to compare the frequency distribution between unmatched groups. *: p<0.05; **: p<0.01; ***: p<0.001; ****: p<0.0001.

REFERENCES

Allin, J.T., and Banks, E.M. (1971). Effects of temperature on ultrasound production by infant albino rats. Dev Psychobiol *4*, 149-156.

Baranek, G.T., Watson, L.R., Boyd, B.A., Poe, M.D., David, F.J., and McGuire, L. (2013). Hyporesponsiveness to social and nonsocial sensory stimuli in children with autism, children with developmental delays, and typically developing children. Dev Psychopathol *25*, 307-320.

Blumberg, M.S., Efimova, I.V., and Alberts, J.R. (1992). Ultrasonic vocalizations by rat pups: the primary importance of ambient temperature and the thermal significance of contact comfort. Dev Psychobiol *25*, 229-250.

Boccaccio, I., Glatt-Deeley, H., Watrin, F., Roëckel, N., Lalande, M., and Muscatelli, F. (1999). The human MAGEL2 gene and its mouse homologue are paternally expressed and mapped to the Prader-Willi region. Hum Mol Genet *8*, 2497-2505.

Boulant, J.A. (1986). Single neuron studies and their usefulness in understanding thermoregulation. Yale J Biol Med *59*, 179-188.

Bumbalo, R., Lieber, M., Schroeder, L., Polat, Y., Breer, H., and Fleischer, J. (2017). Grueneberg Glomeruli in the Olfactory Bulb are Activated by Odorants and Cool Temperature. Cell Mol Neurobiol *37*, 729-742.

Chao, Y.C., Chen, C.C., Lin, Y.C., Breer, H., Fleischer, J., and Yang, R.B. (2015). Receptor guanylyl cyclase-G is a novel thermosensory protein activated by cool temperatures. The EMBO Journal *34*, 294-306.

Chelini, G., Zerbi, V., Cimino, L., Grigoli, A., Markicevic, M., Libera, F., Robbiati, S., Gadler, M., Bronzoni, S., Miorelli, S., *et al.* (2019). Aberrant Somatosensory Processing and Connectivity in Mice Lacking Engrailed-2. J Neurosci *39*, 1525-1538.

Cheng, N., Khanbabaei, M., Murari, K., and Rho, J.M. (2017). Disruption of visual circuit formation and refinement in a mouse model of autism. Autism Res *10*, 212-223.

Corbett, B.A., Mendoza, S., Wegelin, J.A., Carmean, V., and Levine, S. (2008). Variable cortisol circadian rhythms in children with autism and anticipatory stress. J Psychiatry Neurosci *33*, 227-234.

Cypess, A.M., Zhang, H., Schulz, T.J., Huang, T.L., Espinoza, D.O., Kristiansen, K., Unterman, T.G., and Tseng, Y.H. (2011). Insulin/IGF-I regulation of necdin and brown adipocyte differentiation via CREB- and FoxO1-associated pathways. Endocrinology *152*, 3680-3689.

Drapeau, E., Riad, M., Kajiwara, Y., and Buxbaum, J.D. (2018). Behavioral Phenotyping of an Improved Mouse Model of Phelan-McDermid Syndrome with a Complete Deletion of the Shank3 Gene. eNeuro *5*.

Estes, A., Zwaigenbaum, L., Gu, H., St John, T., Paterson, S., Elison, J.T., Hazlett, H., Botteron, K., Dager, S.R., Schultz, R.T., *et al.* (2015). Behavioral, cognitive, and adaptive development in infants with autism spectrum disorder in the first 2 years of life. Journal of Neurodevelopmental Disorders *7*, 24.

Fleischer, J., and Breer, H. (2010). The Grueneberg ganglion: a novel sensory system in the nose. Histol Histopathol *25*, 909-915.

Fountain, M.D., Aten, E., Cho, M.T., Juusola, J., Walkiewicz, M.A., Ray, J.W., Xia, F., Yang, Y., Graham, B.H., Bacino, C.A., *et al.* (2017). The phenotypic spectrum of Schaaf-Yang syndrome: 18 new affected individuals from 14 families. Genet Med *19*, 45-52.

Fujiwara, K., Hasegawa, K., Ohkumo, T., Miyoshi, H., Tseng, Y.-H., and Yoshikawa, K. (2012). Necdin Controls Proliferation of White Adipocyte Progenitor Cells. PLoS ONE *7*, e30948.

Gao, S.-C., Wei, Y.-C., Wang, S.-R., and Xu, X.-H. (2019). Medial Preoptic Area Modulates Courtship Ultrasonic Vocalization in Adult Male Mice. Neurosci Bull.

Grinevich, V., and Stoop, R. (2018). Interplay between Oxytocin and Sensory Systems in the Orchestration of Socio-Emotional Behaviors. Neuron *99*, 887-904.

Harony-Nicolas, H., Kay, M., Hoffmann, J.d., Klein, M.E., Bozdagi-Gunal, O., Riad, M., Daskalakis, N.P., Sonar, S., Castillo, P.E., Hof, P.R., *et al.* (2017). Oxytocin improves behavioral and electrophysiological deficits in a novel Shank3-deficient rat. eLife *6*.

Harshaw, C., Leffel, J.K., and Alberts, J.R. (2018). Oxytocin and the warm outer glow: Thermoregulatory deficits cause huddling abnormalities in oxytocin-deficient mouse pups. Hormones and Behavior *98*, 145-158.

Hashimoto, H., Moritani, N., Aoki-Komori, S., Tanaka, M., and Saito, T.R. (2004). Comparison of ultrasonic vocalizations emitted by rodent pups. Exp Anim *53*, 409-416.

Huang, T.N., Yen, T.L., Qiu, L.R., Chuang, H.C., Lerch, J.P., and Hsueh, Y.P. (2019). Haploinsufficiency of autism causative gene Tbr1 impairs olfactory discrimination and neuronal activation of the olfactory system in mice. Mol Autism *10*, 5.

Jendryka, M., Palchaudhuri, M., Ursu, D., van der Veen, B., Liss, B., Kätzel, D., Nissen, W., and Pekcec, A. (2019). Pharmacokinetic and pharmacodynamic actions of clozapine-N-oxide, clozapine, and compound 21 in DREADD-based chemogenetics in mice. Scientific Reports *9*, 4522.

Kasahara, Y., Sato, K., Takayanagi, Y., Mizukami, H., Ozawa, K., Hidema, S., So, K.-H., Kawada, T., Inoue, N., Ikeda, I., *et al.* (2013). Oxytocin Receptor in the Hypothalamus Is Sufficient to Rescue

Normal Thermoregulatory Function in Male Oxytocin Receptor Knockout Mice. Endocrinology *154*, 4305-4315.

Kasahara, Y., Takayanagi, Y., Kawada, T., Itoi, K., and Nishimori, K. (2007). Impaired Thermoregulatory Ability of Oxytocin-Deficient Mice during Cold-Exposure. Bioscience, Biotechnology, and Biochemistry *71*, 3122-3126.

Kasahara, Y., Tateishi, Y., Hiraoka, Y., Otsuka, A., Mizukami, H., Ozawa, K., Sato, K., Hidema, S., and Nishimori, K. (2015). Role of the Oxytocin Receptor Expressed in the Rostral Medullary Raphe in Thermoregulation During Cold Conditions. Front Endocrinol (Lausanne) *6*, 180.

Klint, T., and Andersson, G. (1994). Ultrasound vocalization is not related to corticosterone response in isolated rat pups. Pharmacol Biochem Behav *47*, 947-950.

Kozlov, S.V., Bogenpohl, J.W., Howell, M.P., Wevrick, R., Panda, S., Hogenesch, J.B., Muglia, L.J., Van Gelder, R.N., Herzog, E.D., and Stewart, C.L. (2007). Nature Genetics *39*, 1266-1272.

Kromkhun, P., Katou, M., Hashimoto, H., Terada, M., Moon, C., and Saito, T.R. (2013). Quantitative and qualitative analysis of rat pup ultrasonic vocalization sounds induced by a hypothermic stimulus. Lab Anim Res *29*, 77-83.

Lee, M.R., Scheidweiler, K.B., Diao, X.X., Akhlaghi, F., Cummins, A., Huestis, M.A., Leggio, L., and Averbeck, B.B. (2018). Oxytocin by intranasal and intravenous routes reaches the cerebrospinal fluid in rhesus macaques: determination using a novel oxytocin assay. Molecular Psychiatry *23*, 115-122.

Lee, S.-Y., Park, S.-H., Chung, C., Kim, J.J., Choi, S.-Y., and Han, J.-S. (2016). Oxytocin Protects Hippocampal Memory and Plasticity from Uncontrollable Stress. Scientific Reports *5*.

Lehmann, J., Russig, H., Feldon, J., and Pryce, C.R. (2002). Effect of a single maternal separation at different pup ages on the corticosterone stress response in adult and aged rats. Pharmacol Biochem Behav *73*, 141-145.

Mamasuew, K., Breer, H., and Fleischer, J. (2008). Grueneberg ganglion neurons respond to cool ambient temperatures. Eur J Neurosci *28*, 1775-1785.

Mamasuew, K., Hofmann, N., Kretzschmann, V., Biel, M., Yang, R.-B., Breer, H., and Fleischer, J. (2011). Chemo- and thermosensory responsiveness of Grueneberg ganglion neurons relies on cyclic guanosine monophosphate signaling elements. Neurosignals *19*, 198-209.

Manning, M., Misicka, A., Olma, A., Bankowski, K., Stoev, S., Chini, B., Durroux, T., Mouillac, B., Corbani, M., and Guillon, G. (2012). Oxytocin and Vasopressin Agonists and Antagonists as Research Tools and Potential Therapeutics: Oxytocin and vasopressin agonists and antagonists. Journal of Neuroendocrinology *24*, 609-628.

Matarazzo, V., and Muscatelli, F. (2013). Natural breaking of the maternal silence at the mouse and human imprinted Prader-Willi locus: A whisper with functional consequences. Rare Dis *1*, e27228.

Matsuo, T., Rossier, D.A., Kan, C., and Rodriguez, I. (2012). The wiring of Grueneberg ganglion axons is dependent on neuropilin 1. Development *139*, 2783-2791.

Meziane, H., Schaller, F., Bauer, S., Villard, C., Matarazzo, V., Riet, F., Guillon, G., Lafitte, D., Desarmenien, M.G., Tauber, M.*, et al.* (2015). An Early Postnatal Oxytocin Treatment Prevents Social and Learning Deficits in Adult Mice Deficient for Magel2, a Gene Involved in Prader-Willi Syndrome and Autism. Biological Psychiatry *78*, 85-94.

Morrison, S.F., and Nakamura, K. (2019). Central Mechanisms for Thermoregulation. Annual Review of Physiology *81*, 285-308.

Murata, Y., Li, M.-Z., and Masuko, S. (2011). Developmental expression of oxytocin receptors in the neonatal medulla oblongata and pons. Neuroscience Letters *502*, 157-161.

Muscatelli, F., Desarménien, M.G., Matarazzo, V., and Grinevich, V. (2017). Oxytocin Signaling in the Early Life of Mammals: Link to Neurodevelopmental Disorders Associated with ASD. In Behavioral Pharmacology of Neuropeptides: Oxytocin, R. Hurlemann, and V. Grinevich, eds. (Cham: Springer International Publishing), pp. 239-268.

Nakayama, T., Eisenman, J.S., and Hardy, J.D. (1961). Single unit activity of anterior hypothalamus during local heating. Science *134*, 560-561.

Oelkrug, R., Polymeropoulos, E.T., and Jastroch, M. (2015). Brown adipose tissue: physiological function and evolutionary significance. Journal of Comparative Physiology B *185*, 587-606.

Orefice, L.L., Zimmerman, A.L., Chirila, A.M., Sleboda, S.J., Head, J.P., and Ginty, D.D. (2016). Cell *166*, 299-313.

Oswalt, G.L., and Meier, G.W. (1975a). Olfactory, thermal, and tactual influences on infantile ultrasonic vocalization in rats. Dev Psychobiol *8*, 129-135.

Oswalt, G.L., and Meier, G.W. (1975b). Olfactory, thermal, and tactual influences on infantile ultrasonic vocalization in rats. Dev Psychobiol *8*, 129-135.

Peñagarikano, O., Lázaro, M.T., Lu, X.-H., Gordon, A., Dong, H., Lam, H.A., Peles, E., Maidment, N.T., Murphy, N.P., Yang, X.W.*, et al.* (2015). Exogenous and evoked oxytocin restores social behavior in the *Cntnap2* mouse model of autism. Science Translational Medicine *7*, 271ra278-271ra278.

Petrikovsky, B., Silverstein, M., and Schneider, E.P. (1997). Neonatal shivering and hypothermia after intrapartum amnioinfusion. The Lancet *350*, 1366-1367.

Quintana, D.S., Smerud, K.T., Andreassen, O.A., and Djupesland, P.G. (2018). Evidence for intranasal oxytocin delivery to the brain: recent advances and future perspectives. Therapeutic Delivery *9*, 515-525.

Robertson, C.E., and Baron-Cohen, S. (2017). Sensory perception in autism. Nature Reviews Neuroscience *18*, 671-684.

Schaaf, C.P., Gonzalez-Garay, M.L., Xia, F., Potocki, L., Gripp, K.W., Zhang, B., Peters, B.A., McElwain, M.A., Drmanac, R., Beaudet, A.L., *et al.* (2013). Truncating mutations of MAGEL2 cause Prader-Willi phenotypes and autism. Nature Genetics *45*, 1405-1408.

Schaller, F., Watrin, F., Sturny, R., Massacrier, A., Szepetowski, P., and Muscatelli, F. (2010). A single postnatal injection of oxytocin rescues the lethal feeding behaviour in mouse newborns deficient for the imprinted Magel2 gene. Hum Mol Genet *19*, 4895-4905.

Schindelin, J., Arganda-Carreras, I., Frise, E., Kaynig, V., Longair, M., Pietzsch, T., Preibisch, S., Rueden, C., Saalfeld, S., Schmid, B., *et al.* (2012). Fiji: an open-source platform for biological-image analysis. Nat Methods *9*, 676-682.

Schreiber, R., Diwoky, C., Schoiswohl, G., Feiler, U., Wongsiriroj, N., Abdellatif, M., Kolb, D., Hoeks, J., Kershaw, E.E., Sedej, S., *et al.* (2017). Cold-Induced Thermogenesis Depends on ATGL-Mediated Lipolysis in Cardiac Muscle, but Not Brown Adipose Tissue. Cell Metabolism *26*, 753-763.e757.

Siemann, J.K., Muller, C.L., Forsberg, C.G., Blakely, R.D., Veenstra-VanderWeele, J., and Wallace, M.T. (2017). An autism-associated serotonin transporter variant disrupts multisensory processing. Transl Psychiatry *7*, e1067.

Siemens, J., and Kamm, G.B. (2018). Cellular populations and thermosensing mechanisms of the hypothalamic thermoregulatory center. Pflugers Arch *470*, 809-822.

Symonds, M.E., Pope, M., and Budge, H. (2015). The Ontogeny of Brown Adipose Tissue. Annual Review of Nutrition *35*, 295-320.

Szentgyörgyi, H., Kapusta, J., and Marchlewska-Koj, A. (2008). Ultrasonic calls of bank vole pups isolated and exposed to cold or to nest odor. Physiology & Behavior *93*, 296-303.

Tan, C.L., Cooke, E.K., Leib, D.E., Lin, Y.-C., Daly, G.E., Zimmerman, C.A., and Knight, Z.A. (2016). Warm-Sensitive Neurons that Control Body Temperature. Cell *167*, 47-59.e15.

Tzabazis, A., Mechanic, J., Miller, J., Klukinov, M., Pascual, C., Manering, N., Carson, D.S., Jacobs, A., Qiao, Y., Cuellar, J., *et al.* (2016). Oxytocin receptor: Expression in the trigeminal nociceptive system and potential role in the treatment of headache disorders. Cephalalgia *36*, 943-950.

Wallis, M. (2012). Molecular evolution of the neurohypophysial hormone precursors in mammals: Comparative genomics reveals novel mammalian oxytocin and vasopressin analogues. Gen Comp Endocrinol *179*, 313-318.

Whittington, R.A., Bretteville, A., Virág, L., Emala, C.W., Maurin, T.O., Marcouiller, F., Julien, C., Petry, F.R., El-Khoury, N.B., Morin, F., *et al.* (2013). Anesthesia-induced hypothermia mediates decreased ARC gene and protein expression through ERK/MAPK inactivation. Scientific Reports *3*, 1388.

Wixson, S.K., and Smiler, K.L. (1997). Anesthesia and Analgesia in Rodents. In Anesthesia and Analgesia in Laboratory Animals (Elsevier), pp. 165-203.

Wu, Z., Xu, Y., Zhu, Y., Sutton, A.K., Zhao, R., Lowell, B.B., Olson, D.P., and Tong, Q. (2012). An obligate role of oxytocin neurons in diet induced energy expenditure. PloS One *7*, e45167.

Xi, D., Long, C., Lai, M., Casella, A., O'Lear, L., Kublaoui, B., and Roizen, J.D. (2017). Ablation of Oxytocin Neurons Causes a Deficit in Cold Stress Response. J Endocr Soc *1*, 1041-1055.

Yahiro, T., Kataoka, N., Nakamura, Y., and Nakamura, K. (2017). The lateral parabrachial nucleus, but not the thalamus, mediates thermosensory pathways for behavioural thermoregulation. Scientific Reports *7*.

Zhu, H., Aryal, D.K., Olsen, R.H.J., Urban, D.J., Swearingen, A., Forbes, S., Roth, B.L., and Hochgeschwender, U. (2016). Cre-dependent DREADD (Designer Receptors Exclusively Activated by Designer Drugs) mice. Genesis *54*, 439-446.

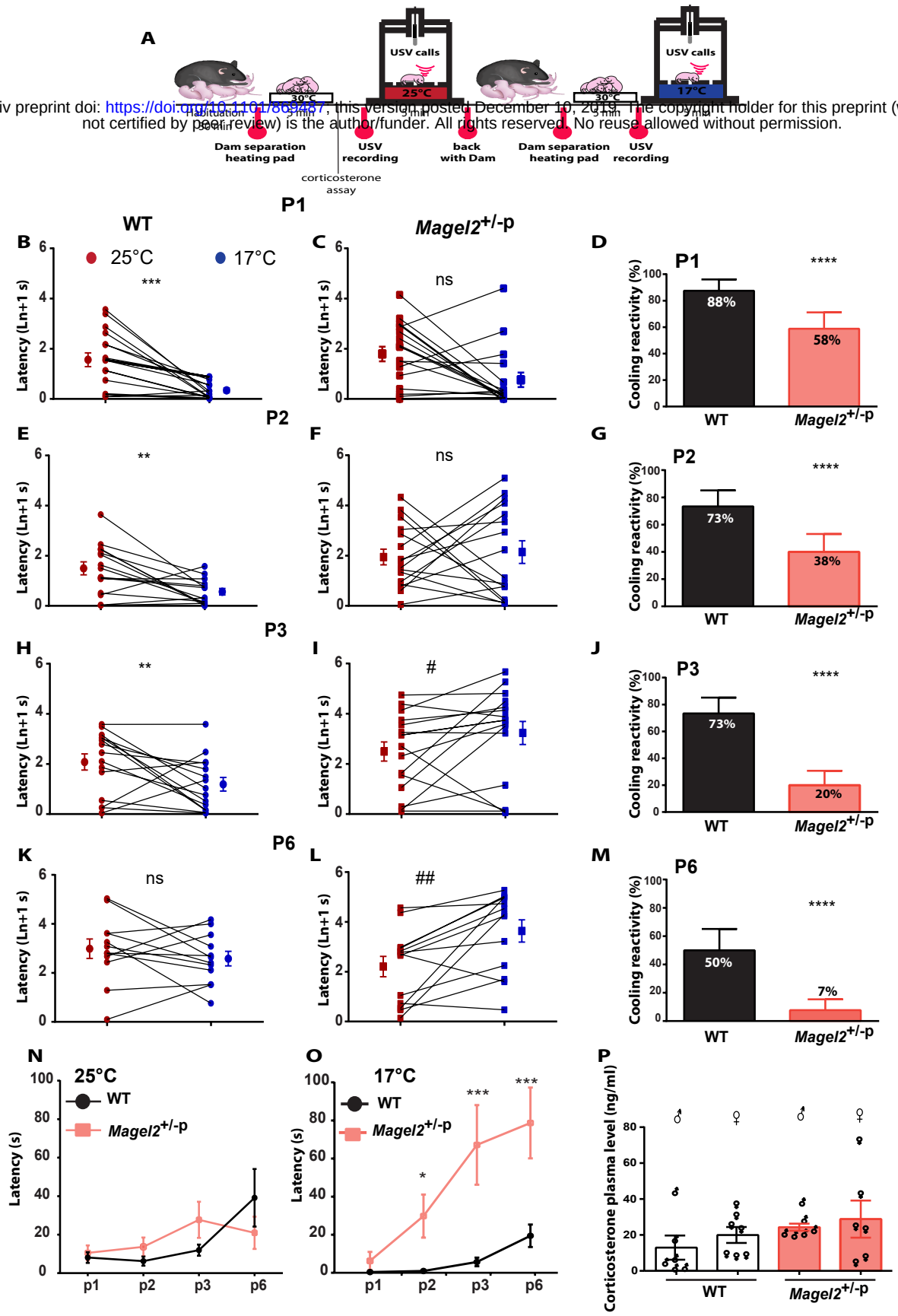

Figure 1. Coolness reactivity failure in Magel2 deficient neonates

A : Experimental procedure. After room habituation, neonates are separated from the dam, placed on a heating pad and each pup is isolated for USVs recording at 25°C for 5 minutes. This procedure is repeated a second time except that the USV chamber is at 17°C. This procedure was reconducted from P1 to P6 in WT and Magel2+/-p neonates. Before/after graphs illustrating the latency to the first call measured upon exposure at 25°C (red dots) followed by 17°C (blue dots) in WT (B;E;H;K) and in Magel2+/-p (C;F;I;L). D;G;J;M: Bar graphs showing animals responsive rate of coolness-stimulated USV in WT and Magel2+/-p neonates from P1 to P6. N-O: Comparison of the latencies to the first call over the age between WT and Magel2+/-p neonates at 25°C (N) and 17°C (O). P: Corticosterone plasma levels in female and male of WT and Magel2+/-p measured when neonates are being isolated for USV calls. Data are presented as mean±SEM, *: $p<0.05$; **: $p<0.01$; ***: $p<0.001$; ****: $p<0.0001$; #: $p<0.05$; ##: $p<0.01$; ns: non-significant

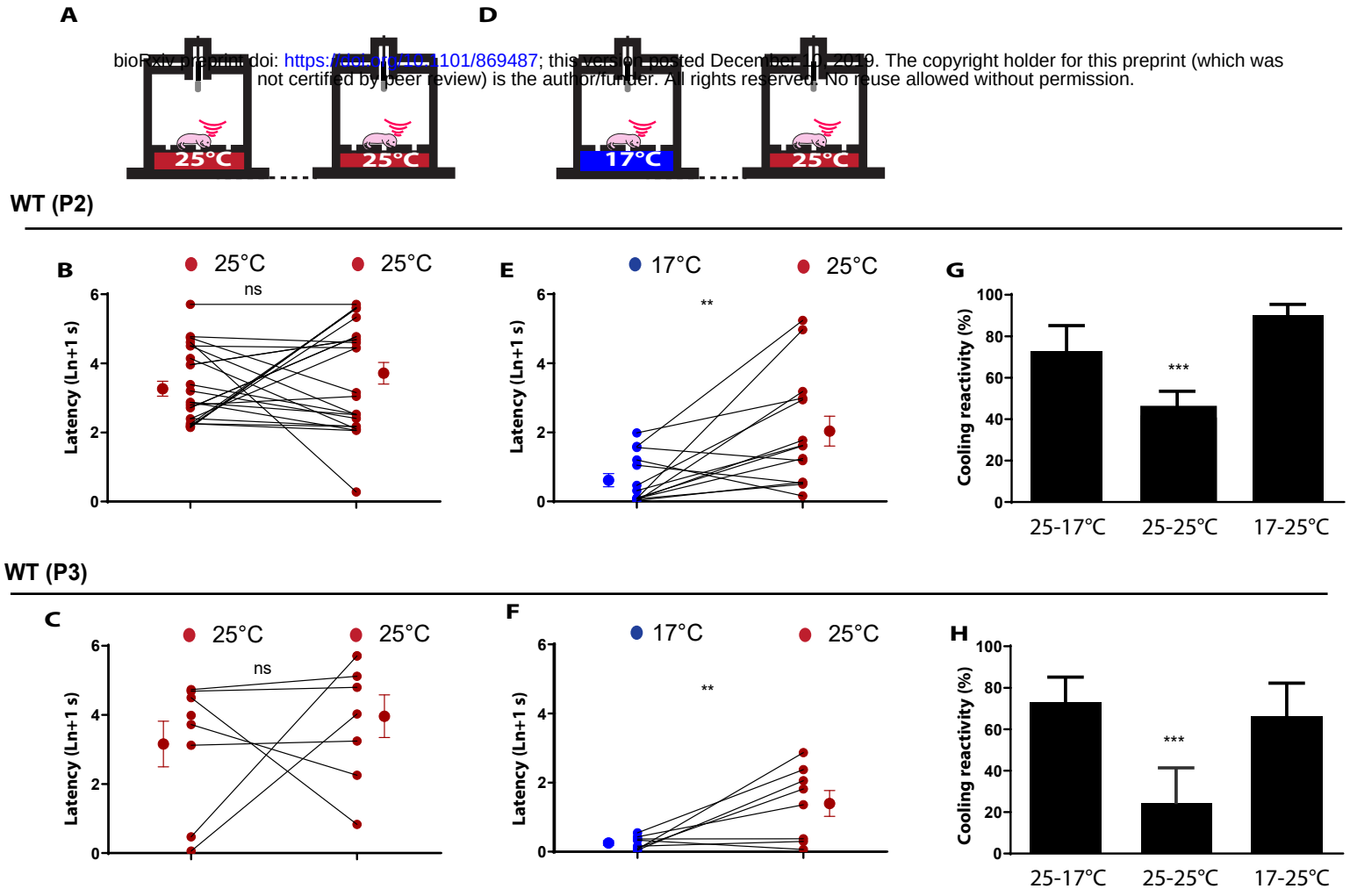

Figure 1- Supplemental 1. Coolness reactivity in WT upon repeated or inversion temperature exposures
A-C : Before/after graphs illustrating the latency to the first call measured upon a repeated exposure at 25°C (blue dots) in WT at P2 (B) and P3 (C). D-F: Before/after graphs illustrating the latency to the first call measured upon exposure at 17°C (red dots) followed by 25°C (blue dots) in WT at P2 (E) and P3 (F). G-H: Bar graphs showing WT animals responsive rate of coolness-stimulated USV at P2 (G) and P3 (H). Data are presented as mean±SEM **: p <0.01; ***: p<0.001; ns: non-significant.

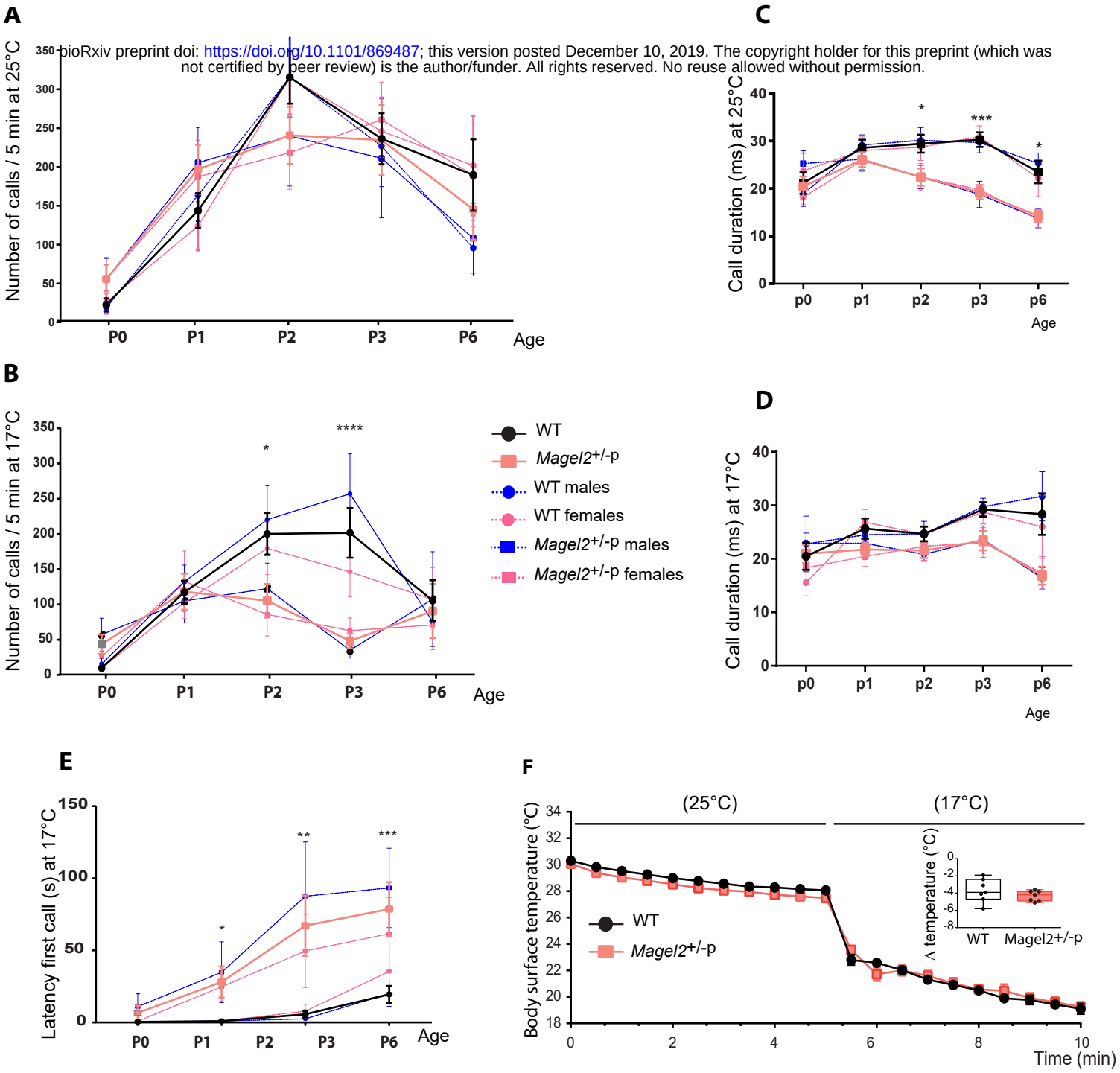

Figure 1- Supplemental 2. Coolness-induced ultrasonic vocalisations (USV) and acute change in skin body temperature in WT and Magel2+/-p.

A-B : Total number of calls over the age in WT and Magel2+/-p at 25°C (A) and 17°C (B). C-D: call duration means of a single call over the age at 25°C (C) and 17°C (D) in WT and Magel2+/-p. Values of male and female (dashed lines) of both WT and Magel2+/-p are plotted for each graph. F: Time course change of body skin temperature in WT (black line) and Magel2+/-p (red line) P2 neonates during 5 minutes at room temperature (25°C) and 5 minutes at 17°C. B: Surface body temperature loss before (at 5 min) and after cool exposure (at 10 min) in WT and Magel2+/-p P2 neonates. Data are presented as Median (with inter-quartile range). Data are presented as mean±SEM *: p<0.05; **: p <0.01; ***: p<0.001; ****: p<0.0001.

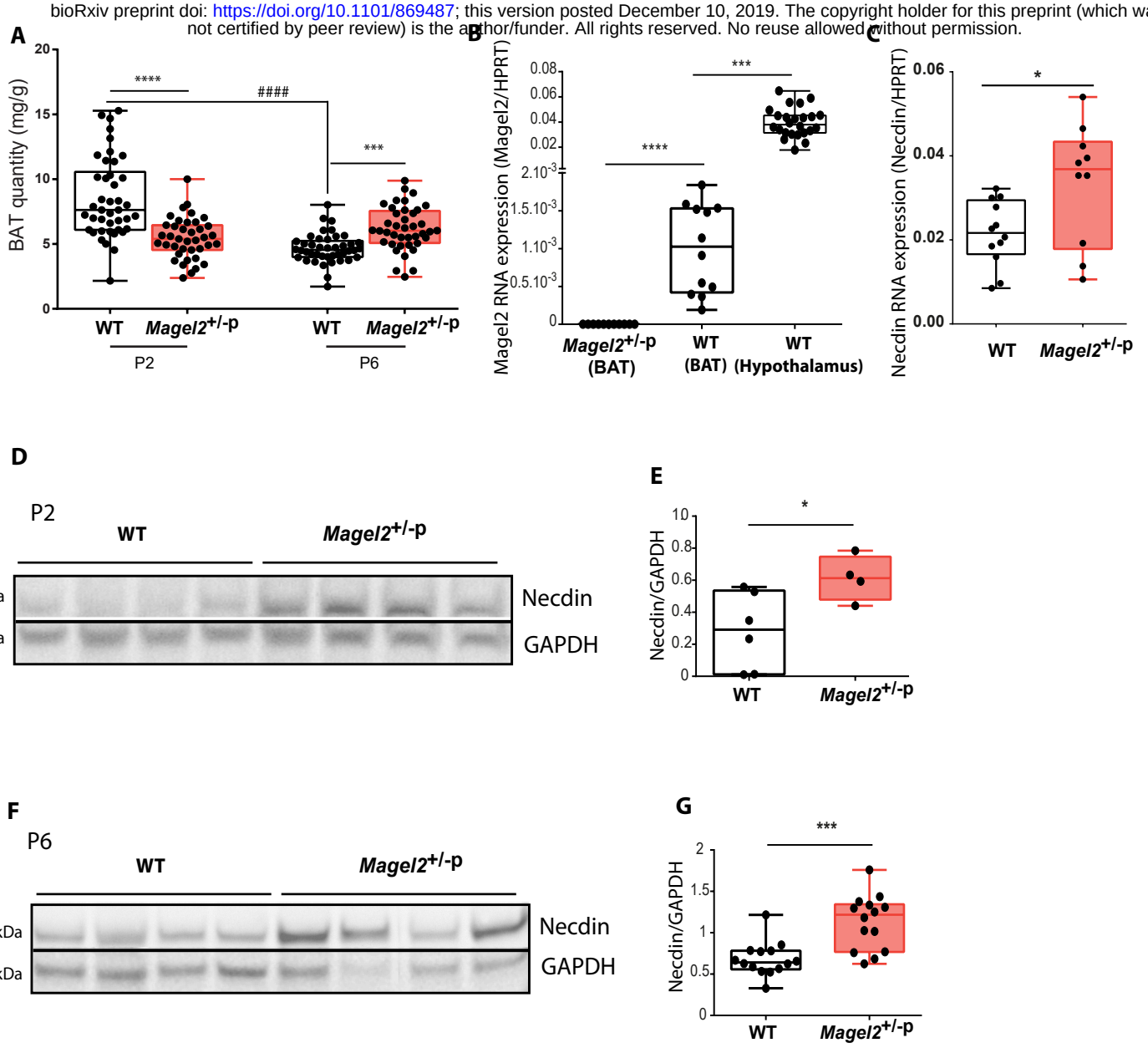

Figure 2. Brown adipose tissue and temperature investigation in WT and Magel2+/-p.
A: Brown adipose tissue (BAT) weight in WT and Magel2+/-p at P2 and P6. B: Quantification of Magel2 RNA transcripts in WT and Magel2+/-p in BAT and hypothalamus at P2. C: Quantification of Necdin RNA transcripts in WT and Magel2+/-p in BAT at P2. D-G: Immunoblot analyses (D-F) and quantification (E-G) of Necdin in BAT at P2 (D-E) and P6 (F-G). Data are presented as median (with interquartile range) *: p<0.05; **: p<0.01; ***: p<0.001; **** or ####: p<0.0001;(* between genotype; # intragenotype).

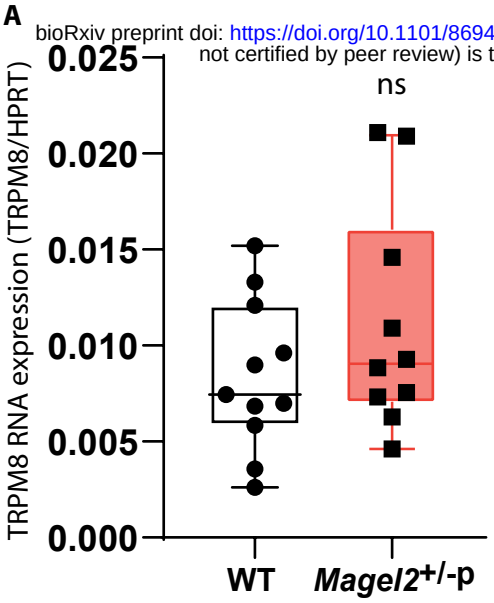

Figure 2- Supplemental 1. mRNA expression of TRMP8

A: Quantification of TRPM8 RNA transcripts in Dorsal root ganglia of WT (n=11) and Magel2+/-p (n=10) at P2

ns: non significant.

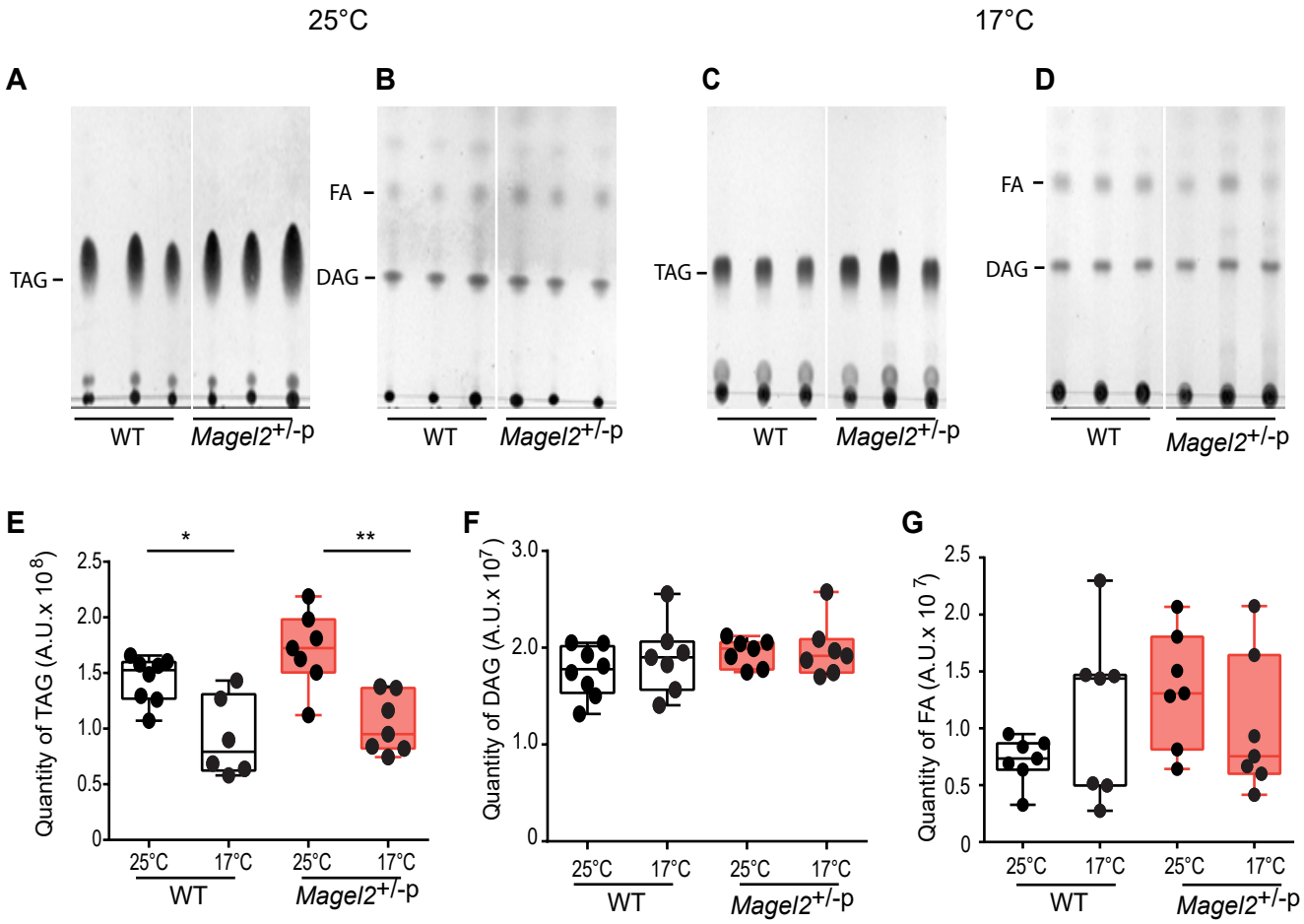

Figure 3. Brown adipose tissue lipids after cool exposure in WT and Magel2+/-p.
A-D: Total lipid extraction of WT and Magel2+/-p BAT and thin layer chromatography analysis of TAG, DAG and FA. E-F-G: Quantifications of TAG (C), DAG (D) and FA (E) Data are presented as median (with interquartile range), *: $p<0.05$; **: $p<0.01$.

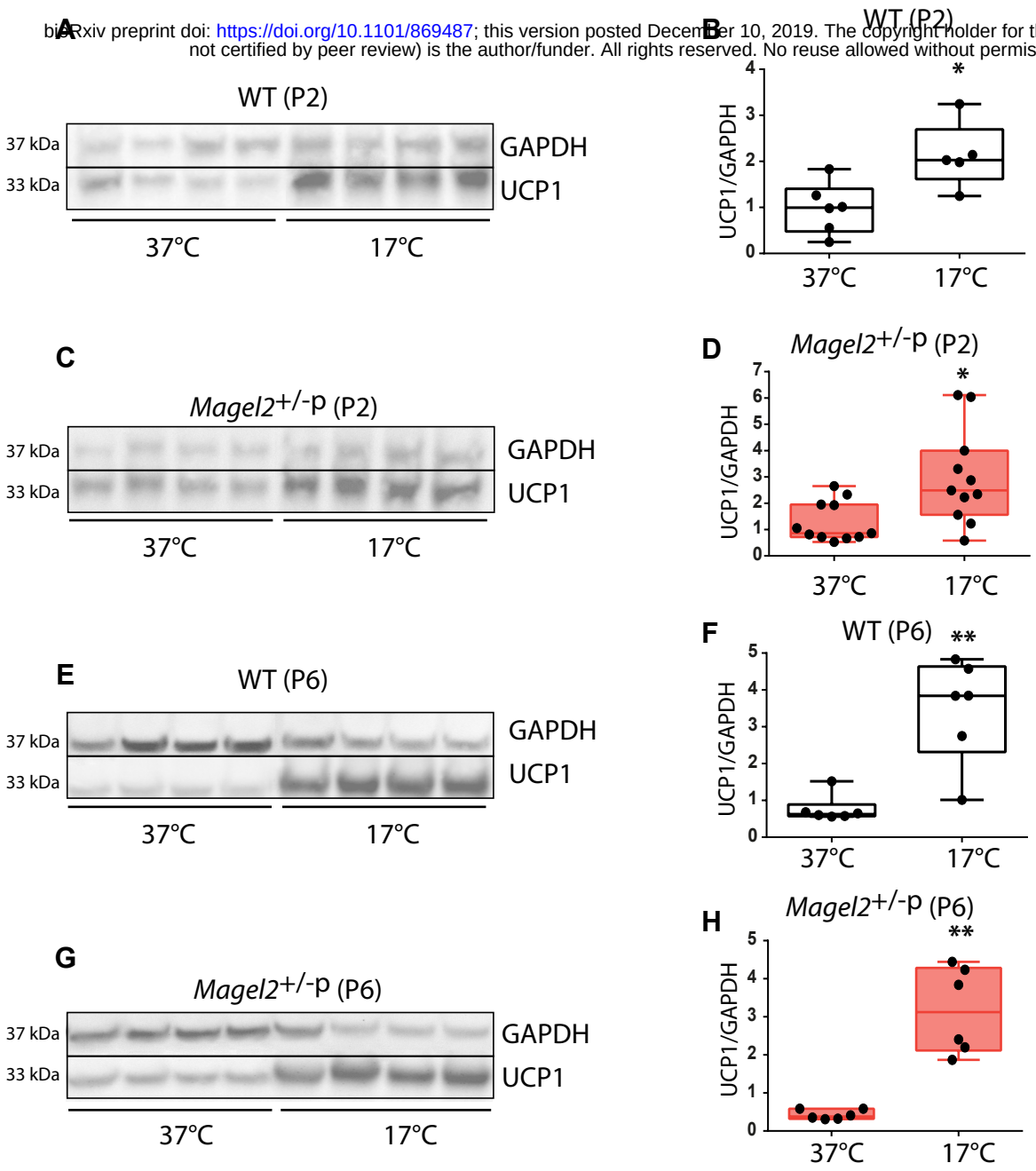

Figure 4. Expression of UCP1 in the brown adipose tissue after cool exposure in WT and Magel2+/-p. Immunoblot analyses and quantifications of UCP1 expression after cool exposure at P2 (A-D) in WT and Magel2+/-p (respectively A -B and C-D) and at P6 (E-H) in WT and Magel2+/-p (respectively E -F and G-H). Data are presented as median (with interquartile range), *: $p<0.05$; **: $p<0.01$.

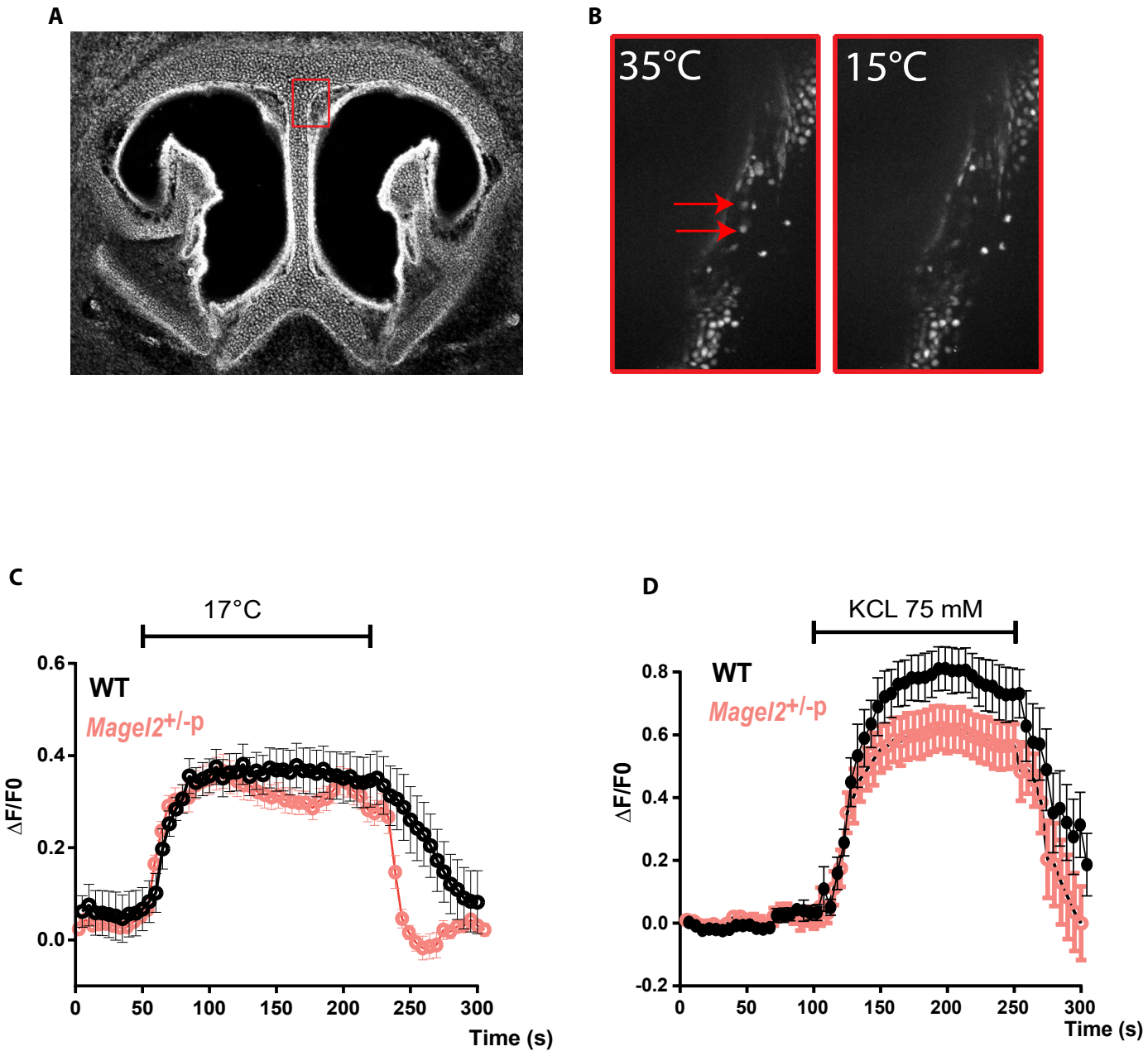

Figure 5. Coolness induced response in the Grueneberg Ganglion (GG) of Magel2+/-p.
A: Coronal sections of the nasal cavity of a P2 mouse with localisation of the GG (red box). B: Inserts represent calcium imaging responses after cool exposure. C: Representative Ca2+ signals induced by cooling from 35°C to 15°C in WT (n=8) and Magel2+/- p (n=9) GG neurons (respectively black and red). D: Representative Ca2+ signals induced in GG neurons by perfusion with KCl (75 mM) were used as a control for viability and responsiveness of tissues slices in WT (n=10) and Magel2+/-p (n=11) GG neurons. ΔF represents change in the ratio of the fluorescence intensity; Data are represented as Mean±SEM.

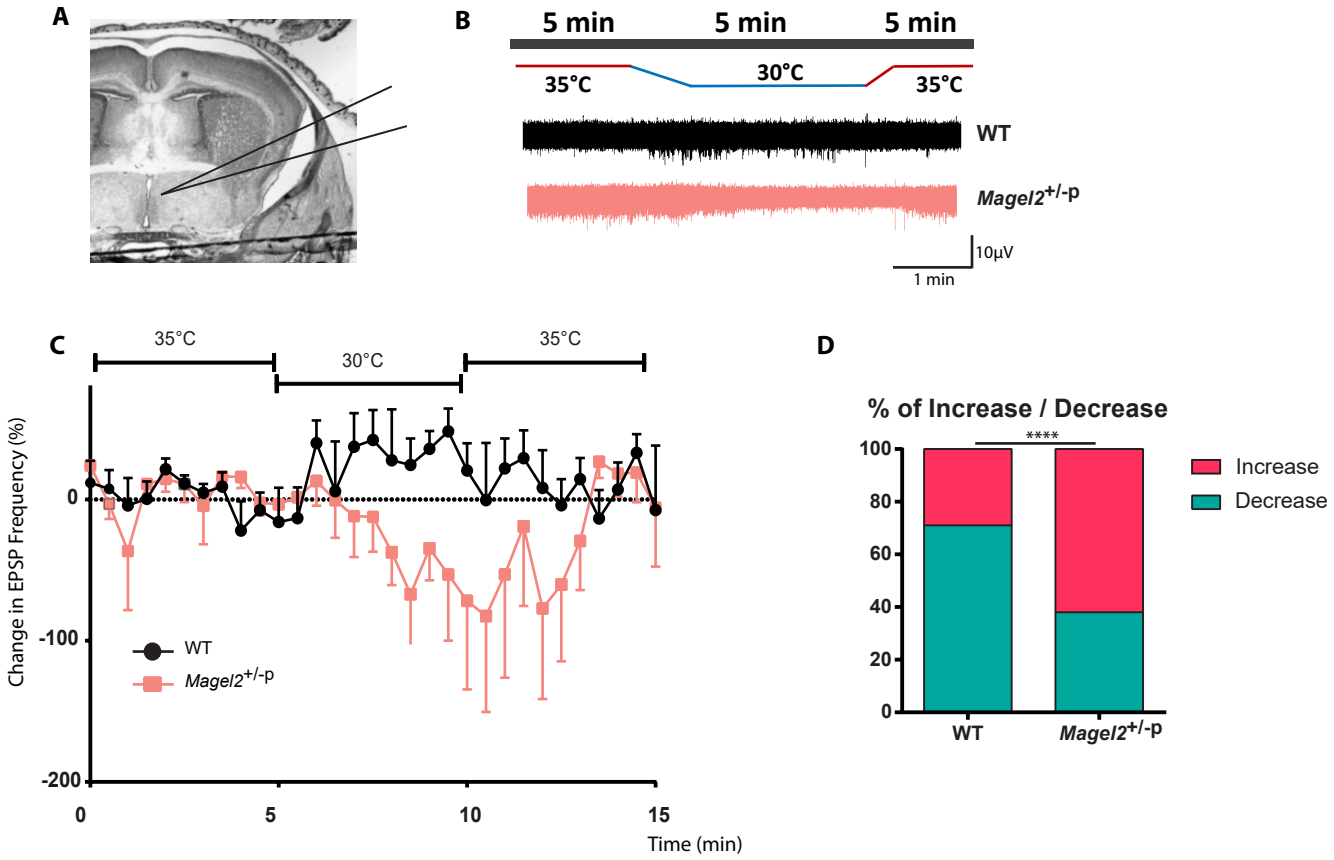

Figure 6. Extracellular field recording in median preoptic area of WT and Magel2+/-p.
A: Localization of the area of recording in the mPOA on P2 mice coronal slice. B: Extracellular field recordings of multiunit activity in the POA of WT and Magel2+/-p mice at P2 before during and after decreasing the temperature of the perfusion medium from 35°C to 30°C. C: Normalized multiunit activity frequency against time. D: Percentage of animals showing an increase or a decrease of multiunit activity in response to a 5°C drop in temperature of the perfusion medium. ****: p<0.0001

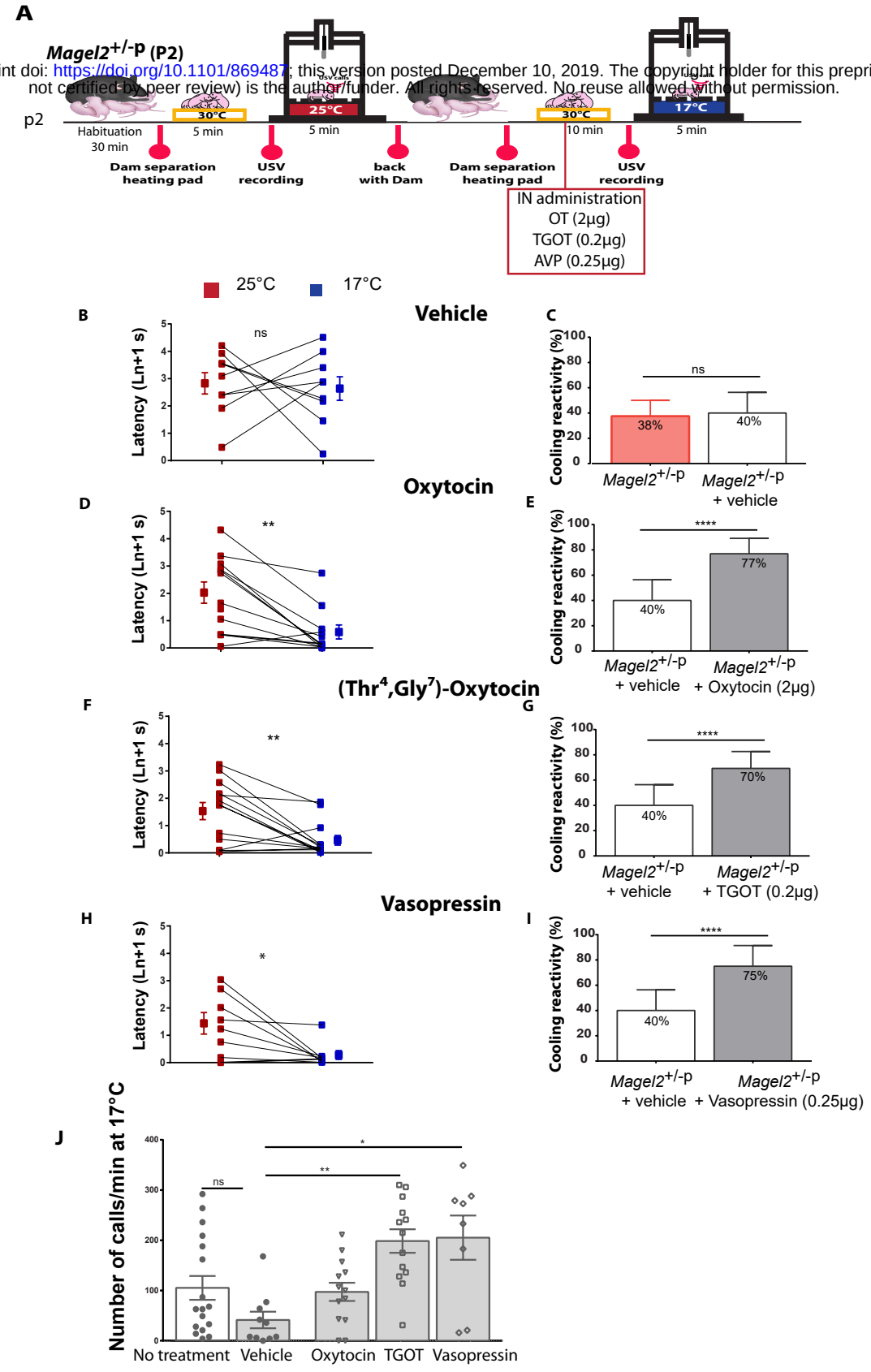

Figure 7. Intranasal oxytocin and oxytocin receptor agonists rescue coolness reactivity in Magel2+/-p.

A: Experimental procedure. After room housing, Magel2+/-p neonates (P2) are separated from the dam, placed on a heating pad and each pup is isolated for USVs recording at 25°C for 5 min. Before repeating the procedure at 17°C and 10 min before the recording, neonates receive an intranasal injection (IN) of Vehicle (NaCl), or Oxytocin (OT, 2 µg) or (Thr^4,Gly^7)-Oxytocin (TGOT, 0.2 µg) or Vasopressin (AVP, 0.25 µg). B-D-F-H: Before/after graphs represent the latency to the first call measured at 25°C (red dots) and 17°C (blue dots) in Magel2+/-p vehicle (B) or treated animals with OT (D), TGOT (F) and AVP (H). C;E;G;I: Bar graphs showing animals responsive rate of coolness-stimulated USV in Magel2+/-p treated with vehicle (C), OT (E), TGOT (G) and AVP (I). J: Total number of calls recorded during 5 minutes in Magel2+/-p treated animals. Data are presented as mean±SEM, *: $p<0.05$; **: $p<0.01$; ***: $p<0.001$; ****: $p<0.0001$.

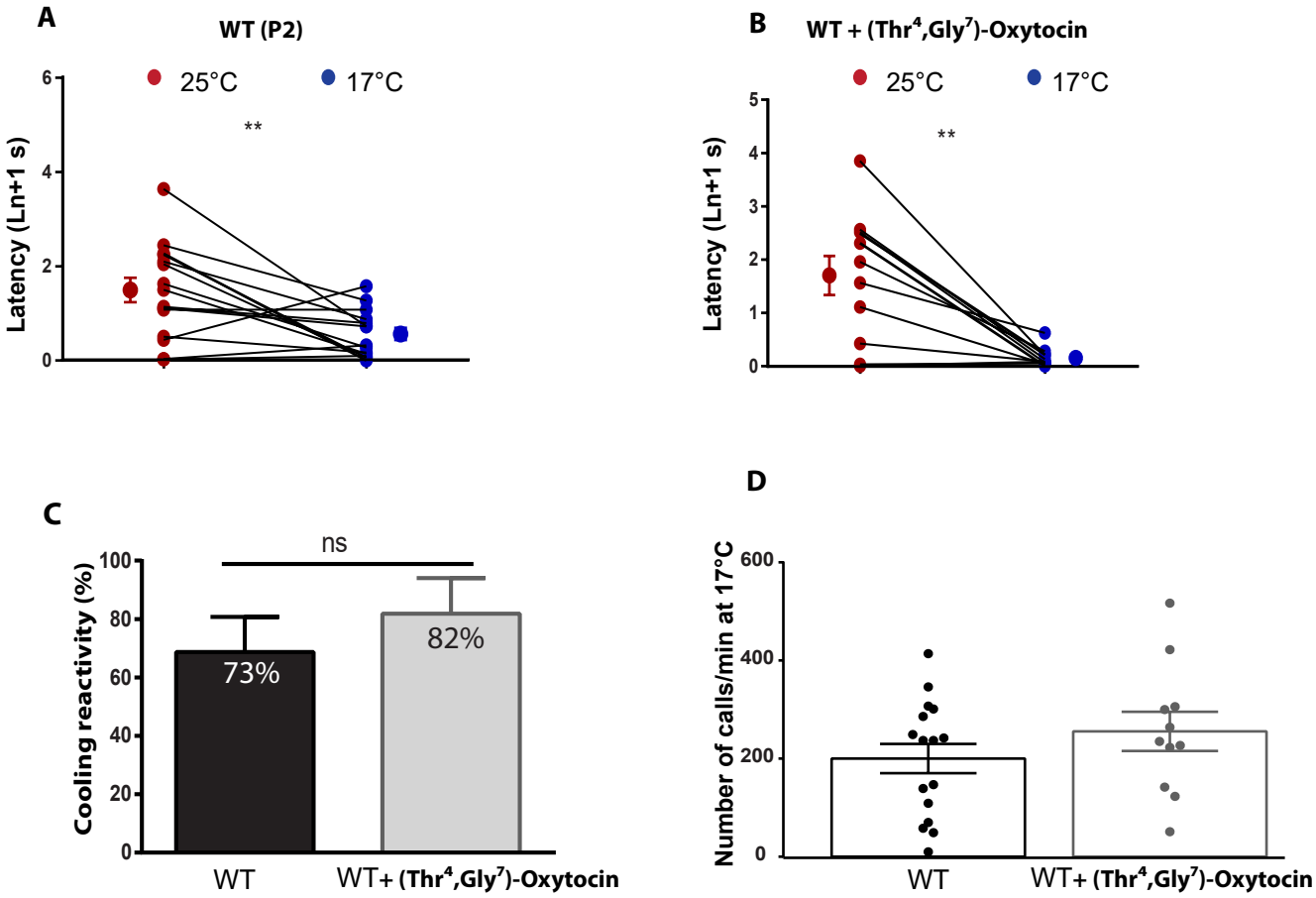

Figure 7 Supplemental 1. Coolness reactivity in WT after an acute TGOT
A-B: Latency for first call before and after cool exposure in untreated (A) or TGOT-treated WT (B). C: Bar graphs showing animals responsive rate of coolness stimulated USV in untreated and TGOT-treated WT. D : Bar graphs showing the total number of calls in WT neonates treated or not with TGOT at 17°C **: $p<0.01$; ns : non significant.

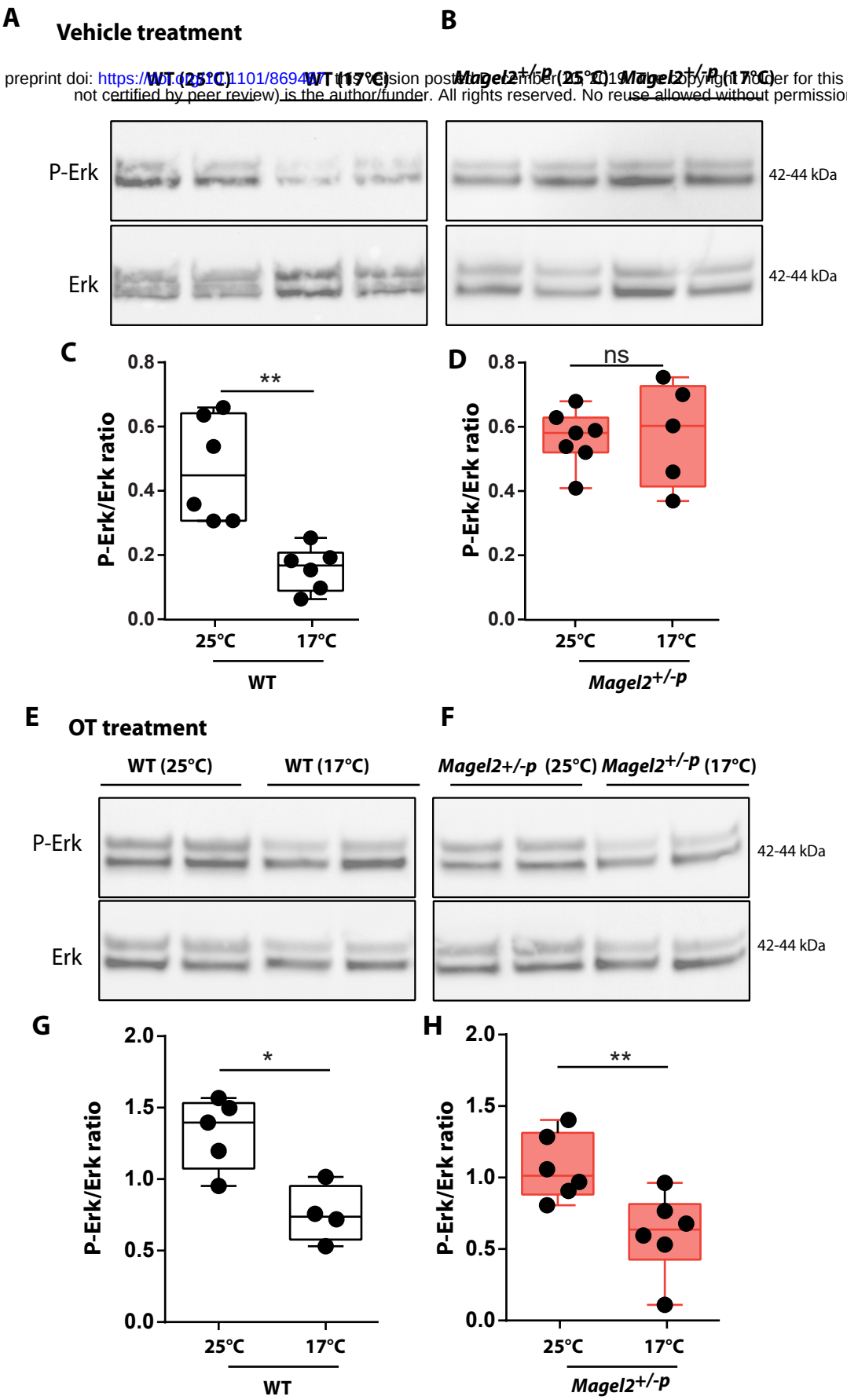

Figure 8. Extracellular signal-regulated kinase (ERK) signaling after cool exposure and Oxytocin treatment. A-B: Representative Western blots of Brain ERK and phosphorylated ERK (pERK) issued from vehicle-treated WT (A) and Magel2+/-p (B) exposed to 25 or 17°C. C-D: Western-blots quantification from WT (C) or Magel2+/-p (D). E-F: Representative Western blots of Brain ERK and phosphorylated ERK (pERK) issued from intranasal OT-treated WT (E) and Magel2+/-p (F) exposed to 25 or 17°C. G-H: Corresponding western-blots quantification from WT (G) or Magel2+/-p (H). *: $p<0.05$; **: $p<0.01$; ns: non significant.

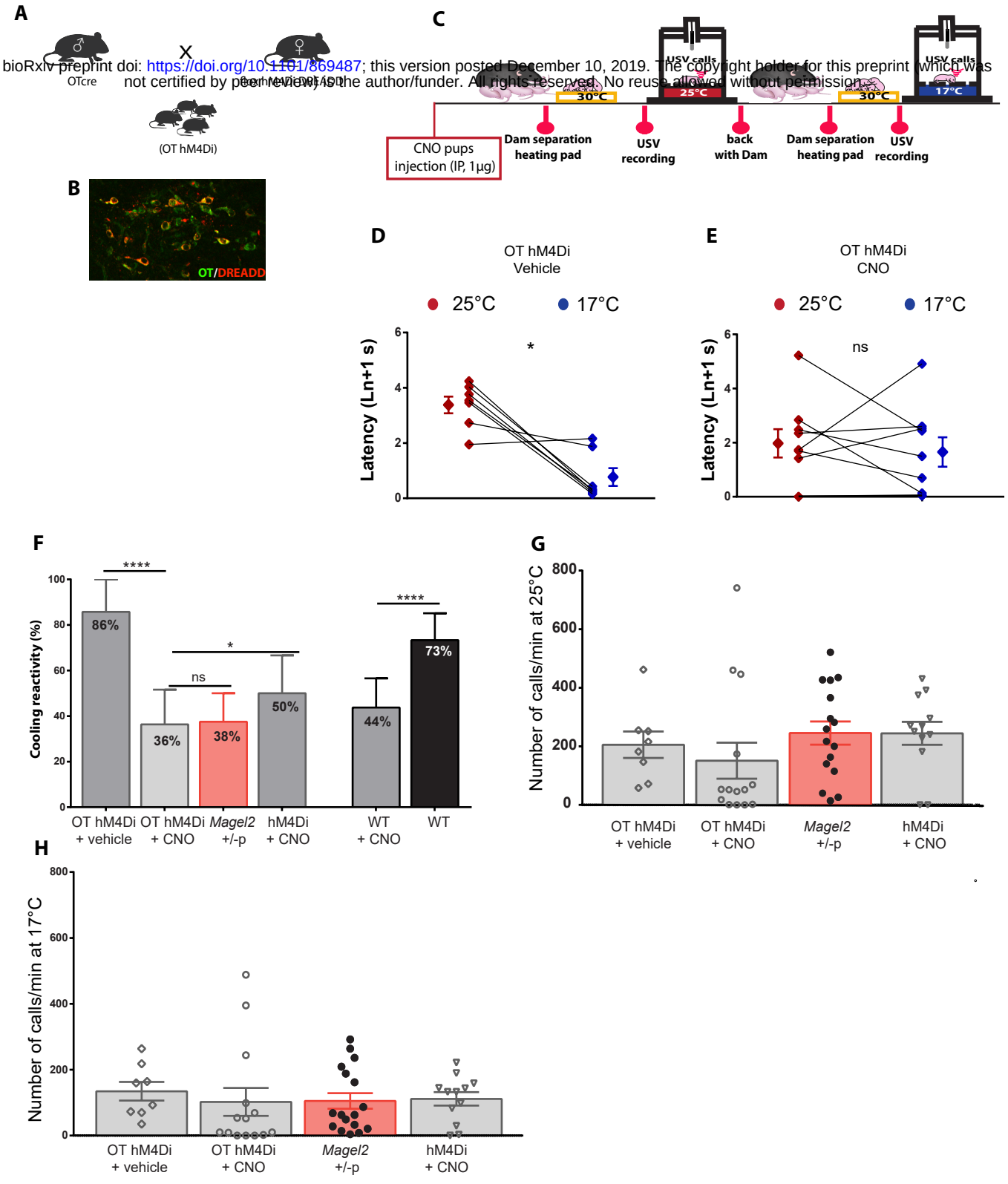

Figure 9. Coolness reactivity failure in WT after oxytocin neurons inactivation.

A: Generation of the hM4Di Dreadd OTCre mice (OT hM4Di). B: Immunohistochemistry illustrating the expression of hM3Di (red) in OT neurons (Green). C: Experimental procedure: IP injection of CNO (1 µg) or vehicle was performed in pups (P2) 2 hours before starting experiment. D-E: Latency for the first call for hm4Di Dreadd OTcre mice treated with vehicle (D) or CNO (E). F: Responsive rate of coolness-stimulated USV in OT hM4Di neonates treated with vehicle or CNO and compared with either Magel2+/-p or neonates non-expressing the hM4Di receptor. The last bar graphs illustrate the effect of CNO treatment on WT neonates. G-H: Total number of calls at 25°C (G) and 17°C (H) in OT hM4Di neonates treated or not with CNO and compared with either Magel2+/-p or neonates non-expressing the hM4Di receptor. Data are presented as mean±SEM *: p<0.05; **: p<0.01; ***: p<0.001; ****: p<0.0001.